Full-length Article

Early life environmental enrichment yields resilience to selected behavioural and brain responses to 5-fluorouracil in mice

Vic K.T. Sun [a,1], Jimmy W.Y. Lam [a], Marcus H.F. Ng [a], Wing-Yan Wong [b,c], William C.S. Tai [b,c,d], Dick H.K. Chow [e,f], Alex K.K. Cheung [a], Benson W.M. Lau [a], Andy S.K. Cheng [a,2], Benjamin K. Yee [a,g,*]

[a] Department of Rehabilitation Sciences, The Hong Kong Polytechnic University, Hong Kong
[b] Department of Applied Biology and Chemical Technology, The Hong Kong Polytechnic University, Hong Kong
[c] The Laboratory for Probiotic and Prebiotic Research in Human Health, The Hong Kong Polytechnic University, Hong Kong
[d] Research Institute for Future Food, The Hong Kong Polytechnic University, Hong Kong
[e] Musculoskeletal Research Laboratory, Department of Orthopaedics and Traumatology, The Chinese University of Hong Kong, Hong Kong
[f] Department of Health Sciences, Hong Kong Metropolitan University, Hong Kong
[g] Mental Health Research Centre, The Hong Kong Polytechnic University, Hong Kong

ARTICLE INFO

ABSTRACT

Chemotherapy remains the primary treatment modality for multiple cancer types, but the cytotoxicity of chemotherapeutic drugs often leads to persistent psychological disturbances that undermine daily function. Minimizing such unwanted effects is challenging in the rehabilitation/prehabilitation of cancer survivors, hence the impetus to identify modifiable external factors capable of improving the recovery process. The importance of social stimulation has been demonstrated in a mouse model showing that grouped housing lowered the likelihood of developing mood disturbance following exposure to chemotherapeutic drugs compared with isolated housing. Social impoverishment thus constitutes a risk factor, and social enrichment may be protective. However, the potential benefits of conventional environmental enrichment that entails extensive sensory and physical stimulation have remained untested in mice. Using C57BL/6 mice, we investigated this research gap by introducing environmental enrichment from an early age (at weaning) to maximize its resilience potential and delaying exposure to the common chemotherapeutic drug, 5-fluorouracil (5-FU), until adulthood (10 weeks old), which comprised six cycles of injections at 40 mg/kg/day × 5 days per fortnight. Our results showed that enriched housing nullified the elevation in anxiety behaviour and proliferation of hippocampal microglial cells caused by chronic 5-FU exposure. Enriched housing also lowered hippocampal IL-17 expression, effectively buffered against the stimulated release of IL-17 by 5-FU. These data extended the potential benefits of social engagement and an active lifestyle in easing the burdens of chemotherapy. Notwithstanding, the negative impacts of 5-FU on hippocampal neurogenesis and musculoskeletal properties were only notable in the enriched mice, suggesting that while environmental enrichment can buffer against certain psychological side effects, the enhanced adaptive plasticity may also increase the susceptibility to specific antineoplastic effects of chemotherapy.

1. Introduction

Living in an enriched environment that offers physical, social, and cognitive stimulation is often associated with enhanced mental capacity and resilience against adverse health factors (Hebb, 1947; Renner and Rosenzweig, 1987; Diamond, 1988; van Praag et al., 2000; Kentner et al., 2016; Kentner et al., 2019). Compared to rodents reared in standard (STD) laboratory housing, those reared in an enriched (ENR) environment have exhibited resilience against cognitive aging (Cotman & Engesser-Cesar 2002; Fernandez-Teruel et al. 1997; Flores-Ramos

---

et al., 2022), genetic risks of Alzheimer's neuropathology (Pietropaolo et al., 2014), the prenatal methylazoxymethanol model of schizophrenia (Zhu & Grace, 2021), and emotional disturbances induced by sleep deprivation (Zhang et al., 2024). Such wide-ranging benefits of ENR housing seen in animals have led to its conceptual incorporation as a viable strategy in neural and psychiatric rehabilitation (Bondi et al., 2014; Raine et al., 2003; McFarlane et al., 2017). While the potential benefits associated with an enriched environment are often attributed to enhanced neural plasticity that facilitates adaptive functional compensation, recent demonstration of resilience to metabolic dysfunction (Kobiec et al., 2023) and cancer (Cao et al., 2010) have suggested the further involvement of interactions with the immune and nervous systems (Dantzer et al., 2008). After demonstrating that social enrichment could attenuate chemotherapy-induced depression-like behaviour in mice, Walker II et al. (2020) went on to show that the protective effect was attributed to increased brain oxytocin release, which in turn suppressed the brain neuroinflammatory response triggered by chemotherapy drugs.

To isolate the influence of social interaction, Walker II et al. (2020) compared mice housed in isolation conditions with those in standard (STD) housing. Consequently, one could argue that the data also suggest that social isolation potentially exacerbates the development of chemobrain syndrome. However, the resilience and vulnerability interpretations of their findings are not mutually exclusive. Both perspectives align with reports that psychosocial support may help attenuate chemobrain syndrome in cancer survivors (Hughes et al., 2014; Reid-Arndt et al., 2010). However, whether the conventional ENR housing may enhance the resilience against the affective side effects of cytotoxic anticancer drugs compared to standard (STD) group housing remains untested. To date, only the cognitive side effects (or chemobrain) of anticancer drugs have been investigated (e.g. Winocur et al., 2012; Winocur et al., 2016). If the availability of social interaction was the sole cause of the affective resilience reported by Walker II et al. (2020), one may not expect the contrast between ENR and STD housing to reveal substantial differences. At the same time, this comparison could evaluate the additional contribution of the non-social elements of ENR housing, although we may not exclude the possibility that such effects (if demonstrated) may be mediated by enhancing the complexity or specific quality of social interaction.

To directly address the unresolved issues, we report here the outcomes of a direct comparison between the effects of conventional enriched (ENR) housing and standard (STD) group housing on the resilience against the psychological side effects of cytotoxic anticancer drugs in mice. This comparison was designed to complement and expand upon the findings of Walker II et al. (2020), because our STD housing procedure essentially resembled the "socially enriched" condition employed in their study. Hence, any resilience effects of ENR housing demonstrated in comparison to STD housing may indicate additional benefits beyond those reported in their study.

Here, we intentionally followed the convention to initiate ENR housing early in life, at weaning age, to maximize its potential benefits. To avoid toxicity to early life development, the cytotoxic anti-cancer agent did not begin until the animals had reached adulthood. 5-fluorouracil (5-FU) was selected as the cytotoxic chemotherapeutic agent due to its well-established antineoplastic and antimetabolite properties, as well as its widespread usage in various forms of human cancer (Longley et al., 2003; WHO, 2020). Here, we opted for a monotherapy approach and emphasized the chronic nature of the 5-FU treatment in human cancer patients that typically entails repeated treatment cycles interspersed with recovery periods (e.g., Salama et al., 2011).

Our experimental design did not intend to model chemobrain syndrome presented against a background or history of malignancy but to isolate the effects attributed solely to chronic 5-FU exposure. Accordingly, we followed Walker II et al. (2020) by employing wild-type mice instead of any murine cancer model. Unlike their emphasis on chemobrain specific to breast cancer survivors, however, our experiment was conducted in male mice instead of ovariectomized female mice.

Behavioural testing was performed in the 9-day recovery period that followed the last two cycles of 5-FU treatment (Fig. 1A). The test battery included assays for emotional, cognitive and motor behaviour. To evaluate possible tolerance to the acute impact of 5-FU, we monitored body weights throughout the study and characterised the diurnal pattern of home cage running in the ENR cages across cycles of 5-FU treatment. We subsequently measured concomitant changes in neural proliferation and immune activation in the hippocampus using immunohistochemistry and immunoassays.

Furthermore, we expanded our investigation to include peripheral tissues known for their adaptive plasticity in response to environmental stimuli and chemotoxicity. However, conducting a comprehensive toxicity profile on multiple organs would far exceed the present scope and our capacity. In particular, the hypothesis that voluntary running can mitigate the catabolic effects of chemotherapy on the musculoskeletal system by promoting metabolic adaptations in muscles and bones (Aires et al., 2024; Kim et al., 2020) encouraged us to examine, for the first time, whether the adverse effects of 5-FU exposure on these tissues could also be attenuated by voluntary wheel running. Our enriched environment was expected to strengthen weight-bearing muscles (Sudo et al., 2023) and increase bone density (Isaksson et al., 2009). To this end, we measured the mass of three lower limb muscles, determined the biomechanical properties of the femur, and performed morphological analysis of soleus muscle fibres. These analyses enabled us to explore the potential protective effects of physical activity on musculoskeletal health during chemotherapy, even though the present study did not constitute a standard model of cancer-related cachexia.

2. Methods

2.1. Subjects

All mice in this study originated from breeders of the inbred C57BL/6J strain from Jackson Laboratory (USA) in the Central Animal Facilities (The Hong Kong Polytechnic University). We collected forty male mice from ten independent multiparous litters born within three days of each other, which were weaned and rehoused on the same day, i.e., between postnatal days 21 and 23. Four male pups from each litter were randomly distributed to one of four conditions according to a 2 × 2 (Housing × Chemo) randomized block design (N = 10 per condition).

In this study, we selected C57BL/6J mice rather than Balb/C mice (cf. Walker et al., 2020) because C57BL/6J is more commonly used in murine behavioral studies. Our choice of male mice also deviated from Walker et al. (2020), who employed female mice that were ovariectomized 'to eliminate the confound of acute ovarian failure in response to chemotherapy administration' (*pp.* 452). We refrained from strictly following Walker et al. (2020) due to concerns that an abrupt menopausal state in young female adults could limit the generalization of broader conclusions across various cancer types affecting both women and men at different ages. Given our limited time and breeding capacity, which prevented us from securing sufficient litters with four male and four female pups each, we decided to study male mice first. This choice had the advantage of minimizing irreversible chemotherapy side effects on reproductive organs and allowed us to avoid confounds related to the female reproductive cycle. We reserve the possibility of repeating the experiments with female mice in the future to explore sex-related physiological and hormonal differences, including oxytocin-dependent regulation of anxiety behaviour (see, Li et al., 2016), which Walker et al. (2020) emphasized as a potential mediator of chemotherapy-induced mood changes.

The two *Housing* conditions contrasted enriched (ENR) housing and standard (STD) housing, while the two *Chemo* conditions were chronic 5-fluorouracil (5-FU) treatment and vehicle treatment. The University's Animal Subjects Ethics Committee (#16–17/45-RS-R) approved all procedures specified in this study. The treatments and manipulations
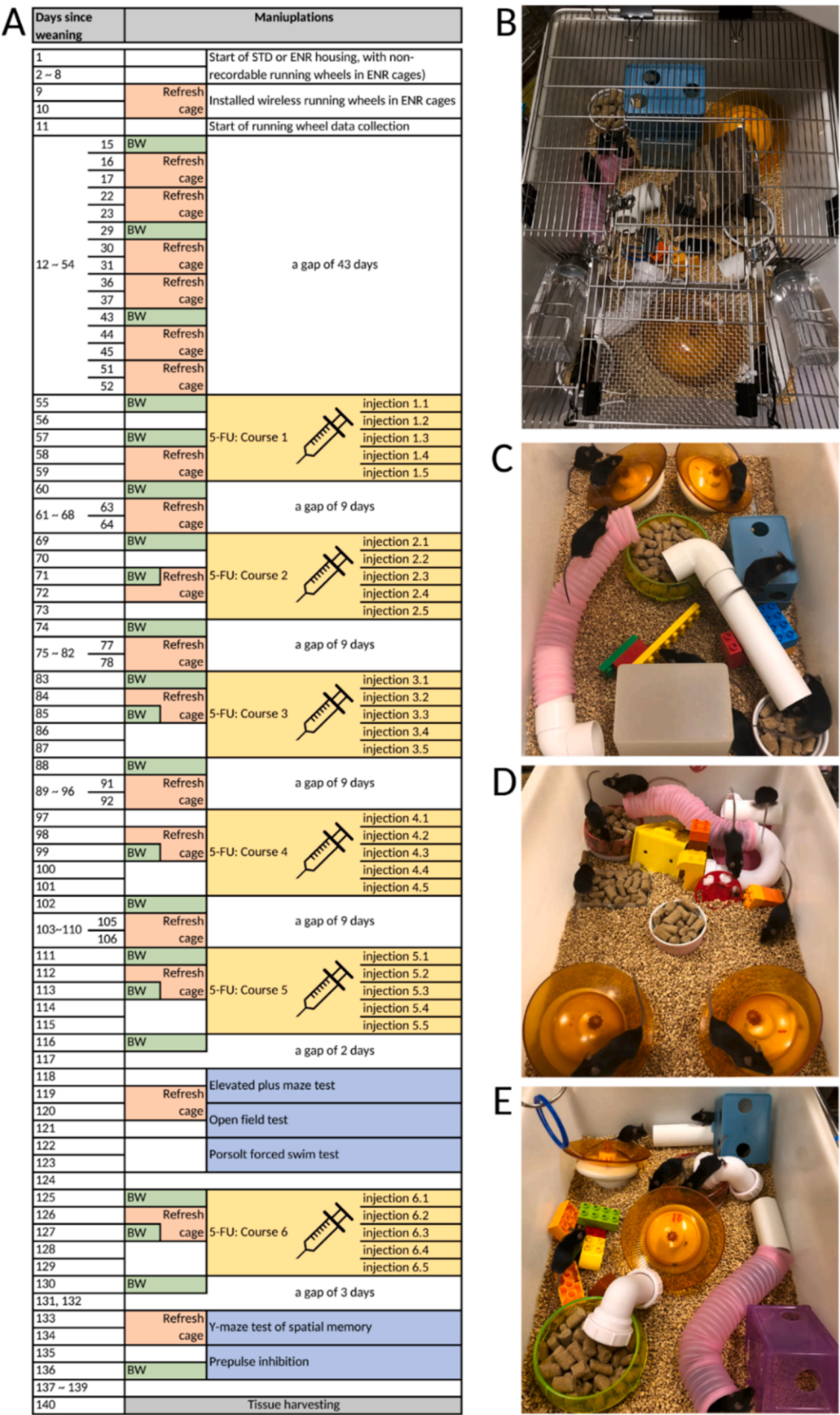
A

Days since weaning			Maniuplations	
1			Start of STD or ENR housing, with non-recordable running wheels in ENR cages)	
2 ~ 8				
9		Refresh	Installed wireless running wheels in ENR cages	
10		cage		
11			Start of running wheel data collection	
12 ~ 54	15	BW	a gap of 43 days	
	16	Refresh		
	17	cage		
	22	Refresh		
	23	cage		
	29	BW		
	30	Refresh		
	31	cage		
	36	Refresh		
	37	cage		
	43	BW		
	44	Refresh		
	45	cage		
	51	Refresh		
	52	cage		
55		BW		injection 1.1
56				injection 1.2
57		BW	5-FU: Course 1	injection 1.3
58		Refresh		injection 1.4
59		cage		injection 1.5
60		BW	a gap of 9 days	
61 ~ 68	63	Refresh		
	64	cage		
69		BW		injection 2.1
70				injection 2.2
71		BW Refresh	5-FU: Course 2	injection 2.3
72		cage		injection 2.4
73				injection 2.5
74		BW	a gap of 9 days	
75 ~ 82	77	Refresh		
	78	cage		
83		BW		injection 3.1
84		Refresh		injection 3.2
85		BW cage	5-FU: Course 3	injection 3.3
86				injection 3.4
87				injection 3.5
88		BW	a gap of 9 days	
89 ~ 96	91	Refresh		
	92	cage		
97				injection 4.1
98		Refresh		injection 4.2
99		BW cage	5-FU: Course 4	injection 4.3
100				injection 4.4
101				injection 4.5
102		BW	a gap of 9 days	
103~110	105	Refresh		
	106	cage		
111		BW		injection 5.1
112		Refresh		injection 5.2
113		BW cage	5-FU: Course 5	injection 5.3
114				injection 5.4
115				injection 5.5
116		BW	a gap of 2 days	
117				
118			Elevated plus maze test	
119		Refresh		
120		cage	Open field test	
121				
122			Porsolt forced swim test	
123				
124				
125		BW		injection 6.1
126		Refresh		injection 6.2
127		BW cage	5-FU: Course 6	injection 6.3
128				injection 6.4
129				injection 6.5
130		BW	a gap of 3 days	
131, 132				
133		Refresh	Y-maze test of spatial memory	
134		cage		
135			Prepulse inhibition	
136		BW		
137 ~ 139				
140			Tissue harvesting	

Fig. 1. The timeline of the experiment is tabulated in **(A)** summarizing the maintenance, manipulations, and tests performed. The timeline begins from the day of weaning (as day 1) when the animals were 21–23 days old. On that day, the (male) mice were rehoused in standard (STD) or enriched (ENR) cages (see **Methods**). Each cycle of 5-fluorouracil (5-FU) comprised 5 separate daily injections. The days when body weights were measured are marked by "BW". The days on which the ENR cages were refreshed are also indicated. The modification of the cage top of the ENR cage is illustrated in **(B)**. Examples of the re-arrangement carried out during refreshment to one ENR cage are shown in **(C)** to **(E)**.

were performed under license issued by the Department of Health, Hong Kong, under the Animals (Control of Experiments) Ordinance (Cap. 340). All procedures were approved by the University's Animal Subjects Ethics Committee and conformed to the ethical standards of the European Union's Directive 2010/63/EU and the guidelines published by the US National Academies (2011).

2.2. Housing conditions

A dedicated rack housed all Makrolon® cages (Tecniplast, Italy) in a climatized (22 ± 1°C and 55 ± 5 % RH) vivarium maintained under a 12 h/12 h normal light–dark cycle with lights off from 2000 to 0759 hrs. All animals lived in their respective housing conditions till the end of the experiment. Food and water were available *ad libitum* unless otherwise stated. Cages were renewed weekly. The differential housing closely followed our previous studies (Pietropaolo et al., 2006, 2014).

Mice in the STD condition were kept in cages (EUROSTANDARD TYPE II) that measured 268 × 215 × 141 mm, with a floor space of approximately 370 cm^2. All STD cages had a water bottle and food pellets placed in the designated troughs on the wire top, each holding five mice. In the ENR condition, mice were housed in cages (EUROSTANDARD TYPE VI, model 224 with a raised wire lid) that measured 598 × 380 × 200 mm with a floor space of 1,820 cm^2. Each ENR cage held ten mice and was equipped with various items, such as pet balls, climbing chains, tunnels made from PVC tubes and water hoses, hiding places made from plastic boxes, wooden ladders, and two running wheels. We upgraded the running wheels to low-profile running discs (ENV-047, Med Associates Inc., USA) on the 10th day of differential housing for continuous wireless recording of voluntary running activity. Food pellets were available from bowls placed inside each ENR cage instead of the original drop-in food hopper (access to which was blocked). Water was accessible from two drinking bottles placed on the wire lid. The renewal and relocation of the enrichment items were integral components of environmental stimulation (Renner and Rosenzweig, 1987) and were performed twice weekly. Daily inspections ensured the adequate supply of food and water, and the running wheels were free from any obstruction. Any damaged enrichment items were promptly replaced.

2.3. Chronic 5-fluorouracil regime

The first treatment cycle began 55 days after the initiation of differential housing when all animals were 11 weeks old (Fig. 1A). 5-fluorouracil (5-FU), obtained from Sigma-Aldrich USA (Cat# F6627, HPLC-Grade), was freshly dissolved in sterile 0.9 % NaCl solution on the days of injection. Each cycle comprised five daily intraperitoneal injections of 5-FU at a dose of 40 mg/kg, with mice in the saline condition (ENR/Saline and STD/Saline groups) receiving vehicle saline injections. After the five injections, the mice recovered for nine days before starting the next treatment cycle, with body weights recorded before the first and third injections and 24 h after the fifth injection. Injections were always performed at 1500 hrs, on Monday to Friday. Our choice of the chronic, multi-cycle regimen of 5-FU treatment was consistent with prior studies investigating the effect of chronic 5-FU in C57BL/6 male mice. The specified 2-week cycle period was adopted from a series of studies of 5-FU monotherapy or in combination with another anti-cancer agent (Sougiannis et al., 2019; VanderVeen et al., 2020; VanderVeen et al., 2022a; VanderVeen et al., 2022b). The decision to examine the long-term effect after 5 to 6 treatment cycles was to approximate a human study employing a similar 2-week cycle period of 5-FU in combination with hydroxyurea and radiotherapy in patients with head and neck carcinoma (Salama et al., 2011).

2.4. Behavioural assessment

Five behavioural tests were conducted when the animals were 20 to 23 weeks old (i.e., days 118–123 & 133–136 after differential housing.

See Fig. 1A). The first test was the elevated plus maze (EPM) test to measure anxiety. Next, the open field test evaluated locomotor activity, followed by the Porsolt forced swim test (FST) before the start of the sixth treatment cycle. After the sixth treatment cycle, we conducted the Y-maze test to assess spatial familiarity and prepulse inhibition (PPI) of the acoustic startle reflex. Each test was conducted over two days, with half of the animals in all conditions evaluated each day to ensure that the animals were left undisturbed for at least 24 h between tests. All tests were conducted in dedicated testing rooms between 0900 and 1900 hrs, under dim lighting, and after the animals had acclimated to the room for at least 30 min.

2.4.1. Elevated plus maze

The elevated plus maze (EPM) was constructed of grey acrylic, with four 30-cm arms connected to a 5 × 5 cm central platform elevated 65 cm above the floor. Two opposing arms were enclosed by 30-cm high walls, while the other arms had only a 5-mm border. The mouse was placed in the centre, facing an open arm, and allowed to explore freely for 5 min. Ethovision XT (v11.5, Noldus) tracked the animal's movement to calculate the proportion of time in the open arms and open arm entries as measures of anxiety.

2.4.2. Open field

The open field test was performed in four 40 × 40 cm grey acrylic arenas with 33 cm high walls. Mice freely explored the open field for 30 min, with Ethovision XT tracking the animal's location to compute distance moved and average proximity to the walls in 5-min intervals. The wall-proximity metric was used in preference to time in centre, as it was independent of the size of centre zone.

2.4.3. Y-maze test of spatial familiarity

The Y-maze was constructed of grey acrylic, comprising three 5 cm wide × 30 cm long arms joined at a central triangular region, and a 5-cm high perimeter wall. Retractable doors 5 cm into each arm guided entry. The arm closest to the testing room door was always assigned as the start arm, with the other two designated as familiar (F) and novel (N) arms. The F/N arm configurations were counterbalanced. During the sample phase, the mouse explored the familiar arm for 6 min with the novel arm blocked. The mouse was then moved to an opaque waiting cage in an adjoining room for 30 min. It was then returned to the maze for the 3-min test phase with free access to all arms. Ethovision XT tracked the mouse's location in both phases. Preference for the novel arm was indexed by the ratio (N − F) / (N + F) based on time spent in the arms.

2.4.4. Porsolt forced swim test

The test was conducted using four glass cylinders measuring 15 cm in diameter and 24 cm tall, each filled with 22 °C clean water to a depth of 15 cm. Cardboards separated the glass cylinders from each other to prevent visual contact between mice. The mice were gently descended into the water and observed for 10 min. A camera with a clear side view of all four cylinders recorded all sessions. Ethovision XT was used to obtain immobility time across successive 1-min bins. The Ethovision automated scoring was validated against manual ratings by two blinded observers on the final 6 min of two randomly chosen video recordings.

2.4.5. Prepulse inhibition of the acoustic startle reflex

The test was conducted using a SR-LAB-Startle Response System (San Diego Instruments, USA) equipped with two mouse test chambers as previously described (Sun et al., 2022). Each sound-attenuated chamber contained a non-restrictive cylindrical acrylic enclosure (inner Ø = 3.8 cm, length = 8.9 cm) that held the mouse during the test. The enclosure was fixed horizontally onto a lightweight acrylic platform, and the whole assembly rested on a heavy block fixed to the chamber's base. Startle response was detected by a piezoelectric sensor attached to the enclosure assembly, which converted any force exerted by the animal on the enclosure assembly into electrical signals digitised at 1-ms intervals.

A high-frequency loudspeaker mounted above the enclosure maintained the 65-dB(A) background noise and delivered acoustic stimuli in the form of white noise at the desired intensity and duration with a 0.2 ~ 1.0 ms rise/fall time. A house light mounted in the ceiling provided ambient lighting inside each chamber.

After 2 min of acclimatisation, 112 discrete trials were administered at a 15-s variable (10–20 s) inter-trial interval. All trials followed the same basic temporal structure: a 20-ms prepulse stimulus →an 80-ms inter-stimulus interval →a 40-ms pulse stimulus. The intensity of the prepulse varied between 65, 71, 77 and 83 dB (i.e., +0, +6, +12 or + 18 dB units above the 65-dB background), whereas the pulse stimulus varied between 100, 110, 115 and 120 dB – defined as the pulse stimulus. These parameters yielded 16 prepulse-pulse trial definitions. Prepulse inhibition (PPI) refers to the attenuation of the startle response with increasing intensity of the prepulse, expressed as percent inhibition, relative to the baseline startle response elicited by the pulse stimulus when prepulse was set at + 0 above background (i.e., without a perceptible prepulse). The whole-body acceleration was measured using piezoelectric outputs (in mV) over two 65-ms windows starting from the onset of the prepulse and pulse stimuli in each trial. The calculation of % PPI as a function of prepulse intensity (+6, +12, or + 18 dB units above background) and pulse intensity (100, 110, 115, and 120 dB) only included the middle 96 trials. The initial and final eight trials had the prepulse set at + 0, designed to stabilise the startle response at the beginning, and against which the habituation of the startle response throughout the entire session was assessed.

2.5. Peripheral issues harvesting

Three days after completing the behavioural tests, blood (~1.2 ml) was collected from the mice by cardiac puncture under deep non-surviving anaesthesia induced by sodium pentobarbital (150 mg/kg, i. p.). The mice were decapitated immediately afterwards, and the brains were extracted *in toto*. The left hemisphere was separated and fixed in 10 % neutral buffered formalin until tissue processing and paraffin embedding. The right hippocampus was rapidly removed on ice and snap-frozen immediately in liquid nitrogen and stored at −80 °C until processing. Lower limb muscles, including the soleus (SOL), tibialis anterior (TA), and extensor digitorum longus (EDL) were dissected to determine their mass. The SOL muscle fibres were further subjected to morphometric evaluation because the increase in muscle mass due to enriched environment (ENR) housing was found to be independent of changes in whole body mass. This is unlike the reduction in TA mass due to 5-FU, as explained in Section 3.7. This focus also aligned with our *a priori* interest in weight-bearing muscles, which are expected to benefit most from endurance running. Therefore, the soleus muscle was chosen for the morphometric analysis of muscle fibres.

2.6. Immunoassay of immune cytokines in the hippocampus

The frozen right hippocampus was powdered in liquid nitrogen using pestles and mortars, then lysed with 100 μL lysis buffer (Bio-Plex® Cell Lysis Kit #171304011) and homogenized using a Kimble® Pellet Pestle® homogenizer at 2,000–3,000 rpm for 30 s. The homogenate was incubated on ice for 30 min and then centrifuged at $12,000 \times g$ for 30 min at 4 °C. The supernatant was separated into aliquots, snap-frozen, and stored at −80 °C until analysis. One aliquot was thawed on ice, and the total protein concentration was determined using the Bio-Rad Quickstart™ Bradford protein assay. Sample dilution was optimized for lysis buffer/matrix interference with pooled protein extracts from each group. Individual samples were diluted 80 × to determine sample concentration (mean ± SEM = 10.26 ± 4.72 mg/ml, N = 40). Concentrations of immune cytokines—IL-1β, IL-6, IL-10, IL-17A, IFNγ, and TNFα—were measured using the Bio-Plex Pro™ Mouse Cytokine Th17 Panel A 6-Plex Immunoassay kit (#M6000007NY). Following the manufacturer's recommendation, the protein extracts were further diluted

and standardized to 1 mg/ml (50 μL/well) with the supplied sample diluent and 0.5 % v/v bovine serum albumin (from a 15 % w/v stock in ddH2O, Sigma-Aldrich). Reconstituted standards were diluted at a 4 × serial dilution (S1-S8) with the diluent supplied. All washing steps were completed with a Bio-Plex® handheld magnetic washer (#171020100). All samples, including standards, were run in duplicates on the same plate. They were incubated with magnetic beads in a 96-well plate at 25 °C for 30 min under agitation (850 rpm, Eppendorf® ThermoMixer® C). The bead-analyte complex was incubated with detection antibody (30 min, 25 °C, 850 rpm) and SA-PE (10 min, 25 °C, 850 rpm), with 3 × washes after each incubation. The wells were then reconstituted in 125 μL assay buffer and analysed using a Bio-Plex 200 System array reader. Standard curves of individual cytokines were estimated using a 5-parameter logistic function (Bio-Plex Software). Cytokine concentrations of individual samples were expressed in pg/ml per 50 μg protein after correction for sample dilution.

2.7. Immunohistochemistry

After dehydration through a graded series of ethanol and clearing in xylene, the formalin-fixed right brain hemispheres were embedded in paraffin: two 90-min cycles followed by one 180-min cycle at 62 °C under vacuum. The hemispheres were then sectioned at 30 μm in the coronal plane using a rotary microtome. The sections were dewaxed, rehydrated, and mounted onto glass slides (IncuPLUS™ Incupath, USA) and left to air dry. Next, the slides were immersed in preheated (95 °C) Envision Flex Target Retrieval Solution (K800421-2, Dako) for 30 min and then cooled for 45 min at room temperature (RT), followed by rinsing in PBS. Following incubation in Dako Peroxidase-Blocking Solution (S202386) for 10 min at RT to stop endogenous peroxidase activity, the slides were then incubated for 60 min at RT with the primary antibodies (suspended in Dako S302283 antibody diluent) at the following concentrations: anti-IBA1, 1:800 (019–19741, Fujifilm Wako) or anti-DCx, 1:1000 (ab18723, Abcam). After washing in buffer (#K800721-2, Dako), the sections were incubated in HRP-labelled polymer conjugated to the secondary antibody (EnVision® Systems, Peroxidase/DAB, Rabbit/Mouse, Dako K5007) for 30 min. Immunoreactivity was visualized using 3,3′-diaminobenzidine (DAB) chromogen. The DAB reaction was terminated in 1–2 min at the desired level of staining by immersion in deionized water.

2.8. Counting of IBA1 and DCx-immunoreactive cells in the hippocampus

Cell counting and morphometric analysis of IBA1- and DCx-immunoreactive (IBA1-ir and DCx-ir) cells were performed in two sections (180 μm apart) in the dorsal hippocampus (1.82 ~ 2.18 mm posterior to bregma according to Franklin et al., 2007) and two sections (180 μm apart) in the ventral hippocampus (3.40 ~ 3.80 mm posterior to bregma) taken from each animal. High-resolution stitched images of the hippocampal formation of all selected sections were acquired with a light microscope (using a 10 × objective) equipped with a motorized stage and a 3-channel (8-bit) digital camera (Nikon's NIS-Elements Viewer). IBA1-ir cells in CA1–CA3 subfields of cornu Ammonis and the dentate gyrus were counted by ImageJ-FIJI (Schindelin et al., 2012) after grayscaling, thresholding, and noise reduction (two iterations of erosion followed by two iterations of dilation), and expressed in cell counts per mm^2. DCx-ir cells within the granular cell layer with a stained soma and an identifiable apical dendrite extending towards the molecular layer were manually counted under blind conditions and expressed as areal density (counts per mm^2).

2.9. Morphometric evaluation of hippocampal immature neurons and microglia

2.9.1. IBA1-positive cells
Two non-overlapping images (0.36 mm wide × 0.24 mm high) of the

selected sections within the hippocampal region were captured using a 40 × objective. The captured images were imported into ImageJ-FIJI for processing and skeleton analysis as described by Young and Morrison (2018). Following preprocessing and image skeletonization, skeletal features of interest—process length and endpoints—were tagged using the "AnalyzeSkeleton" plugin (https://imagej.net/plugins/analyze-skeleton). Fig. 8H illustrates the conversion of one original photomicrograph to its tagged image. The average number of process endpoints and average process lengths per cell were computed. The two morphometric features of IBA1-positive cells may inform a shift of their functional states. Namely, shorter process length and reduced endpoints may indicate a shift towards a M1 (pro-inflammatory) profile while the opposite changes may suggest a M2 (anti-inflammatory) profile. We refrained from relying on these metrics to support the classification of IBA1-positive cells into M1 or M2 phenotypes for the purpose of cell counts due to their overlapping characteristics. Nonetheless, increase in microglial density would be sufficient to index inflammatory activation, especially the immune response that precedes astrogliosis. Although we did not counted astrocytes, IBA1-positive cell counts represent a common index of the brain's inflammatory state. We may not, however, rely on this measure to comment on the extensive interaction between microglia and astrocytes.

2.9.2. Sholl analysis of DCx-ir immature neurons

Two DCx-ir cells from the dorsal hippocampus and four DCx-ir cells from the ventral hippocampus were randomly selected per mouse. Images of these cells were captured using a 40 × objective and imported into ImageJ-FIJI. The outlines of the cells were delineated, and the centre of the soma was marked manually. Subsequently, Sholl analysis was conducted using ImageJ with the following settings: start radius = 10 μm, step size = 10 μm, ending radius = 150 μm, and radius span = 0. The average number of intersections at successive Sholl radii per DCx-ir cell was calculated separately for the dorsal and ventral hippocampus.

2.10. Skeletal muscles

After decapitation, the lower limb muscles (TA, EDL and Soleus) of the left leg were carefully isolated without stretching or touching of its belly. Connected nerves, vessels, and adipose tissues were then removed. The muscles were blot-dried, weighed and, frozen. Morphological analysis was only performed with the soleus muscles (see Section 2.5), which were embedded in OCT compound for cryo-sectioning. Sections of the soleus from three randomly selected mice from each group were processed to identify type I, IIA, and IIB myosin heavy chain (MyHC) proteins by immunohistochemistry, for evaluating myofiber atrophy and type switching, as previously outlined (Sun et al., 2018). Air-dried 7-μm sections of the soleus mid-belly were mounted and post-fixed with 4 % paraformaldehyde. The sections were then permeabilized with 0.1 % Triton X-100 and treated with BlockAid™ Blocking Solution (Thermo Fisher). Primary antibodies obtained from the Developmental Studies Hybridoma Bank (University of Iowa) were used: type I (BA-D5 mouse IgG2b), type IIA (SC-71 mouse IgG1), and type IIB (BF-F3 IgM), diluted to 5 μg/ml with BlockAid™. After washing in PBS, the sections were incubated with fluorescent secondary antibodies from Thermo Fisher against immunoglobulin isotypes: AF350 goat anti-mouse IgG1 (1:200), AF488 goat anti-mouse IgM (1:300), and AF555 goat anti-mouse IgG2b (1:300) in BlockAid™ for 1 h at room temperature. After coverslipping with Dako fluorescent mounting medium, stitched multicolour channel images of the triple-stained sections were captured using an Eclipse 80i microscope equipped with a DS-Ri2 Nikon camera at 10 × magnification and imported to ImageJ-FIJI. The Myosoft ImageJ plugin (available at https://github.com/Hyojung-Choo/Myosoft/tree/Myosoft-hub) was used to compute the number of stained muscle fibres per section and the minimal Feret diameter of individual fibres. The parameters used (range of area = 400 to 4,000 μm², circularity = 0.4 to 1, and min. Feret = 0.5 μm) were optimized using the soleus of a normal

adult mouse as recommended by Encarnacion-Rivera et al. (2020). Fibres displaying multiple stains were classified as "hybrid," while unstained fibres were labelled as "others". Examples of the triple-stained fluorescence photomicrographs can be found in Supplementary Fig. 2.

2.11. Microarchitectural and mechanical analysis of the femur bone

The left femur was assessed using a micro-CT (μCT-40, Scanco Medical, Brüttisellen). The midshaft of the femur was scanned at an isotropic resolution of 10 μm³ with a fixed scan range of 4 mm (Bouxsein et al., 2010; Huang et al., 2018). The scanning parameters included a beam energy of 70 kV, a current intensity of 114 μA, and an integration time of 200 ms. Noise reduction in the imaging data was achieved through 3D Gaussian filtration with a filter width of 1.2 and filter support of 2. Bone was distinguished from marrow and soft tissue using a global segmentation threshold of 165. Bone mineral density (BMD), bone volume (BV), and bone volume to tissue volume fraction (BV/TV) were calculated. For mechanical characteristics, the femur was assessed through a three-point bending test using a Hounsfield universal testing machine (H25KS) fitted with a 50-N load cell (Huang et al., 2016). The bone was positioned horizontally on supports 10 mm apart, with its anterior surface facing upwards. To determine the failure load, energy to failure, and stiffness, a force was applied to the midshaft at a constant displacement rate of 5 mm/min until failure.

2.12. Statistical analysis

The statistical analyses were conducted using SPSS-IBM for Windows (version 26). Conformity to normal distribution of individual data sets was assessed by Shapiro-Wilk test, along with an inspection of the QQ plot, skewness, and kurtosis, before parametric analysis of variance (ANOVA). The logarithmic transformation applied to the startle response (Csomor et al., 2008) and cytokine data sets was instrumental in correcting their intrinsic positive skewness. All ANOVAs included the between-subject factors Housing (ENR vs STD) and Chemo (FU-5 vs Saline), along with within-subject factors specific to each dataset (namely, 1- or 5-min time bins, prepulse intensity, pulse intensity, dorsoventral axis, Sholl radii, or muscle fibre Feret diameters). Supplementary ANCOVAs were utilized to control for body weight as a confounding variable in the analysis of whole-body startle magnitude and individual muscle mass. Statistical significance was determined at a Type-I error rate of 0.05, with effect size reported in η_p^2. Planned comparisons using Fisher's LSD were conducted to assist interpretation of significant interactions involving Housing and Chemotherapy. These included tests to examine the effect of 5-FU within each housing condition and tests of housing effects among animals within the same treatment condition. Tukey's HSD tests were used for unplanned pairwise comparisons. Data are presented as means ± standard error (SE) provided by SPSS for each ANOVA output, or as adjusted means from the ANCOVA output.

3. Results

3.1. Body weights

Two weeks after weaning and relocation to their respective housing, the rate of body weight (BW) gain was clearly slowed down by ENR housing (Fig. 2A). Divergence in BW due to differential housing was already evident before treatment began when BW growth was rapid. A 2 × 2 × 4 (Chemo × Housing × Time) ANOVA of BW (g) from days 15 to 55 since differential housing (but before treatment began) yielded a significant main effect of Housing [$F(1,36) = 13.63$, $p < 0.001$, $\eta_p^2 = 0.28$], Time [$F(3,108) = 738.67$, $p < 0.0001$, $\eta_p^2 = 0.95$], and their interaction [$F(3,108) = 17.86$, $p < 0.0001$, $\eta_p^2 = 0.33$]. Over the treatment period (six cycles of 5-FU), BW gain slowed down in all groups as all mice had reached adult age. Against this background, 5-FU treatment

persistently retarded weight gain in both ENR and STD mice. The separation of BW between mice in the 5-FU and vehicle saline conditions progressively widened over the six treatment cycles (Fig. 2A).

To examine the effect of successive (five daily) injections *within* treatment cycles, BW was expressed as percent of baseline (just before the first injection of each cycle) and collapsed across the six treatment cycles (Fig. 2B). A short-term BW reduction was evident 24 h after the second injection, and it was partially attenuated by ENR housing. As expected, the drop in BW seen after the second injection was more pronounced after 5-FU than saline injections, but this difference was apparent only during the first, fifth and sixth treatment cycles (data not illustrated). These impressions were supported by the $2 \times 2 \times 6$ (Chemo $\times$ Housing $\times$ Treatment Cycles) ANOVA of %BW 24 h after the second injection, which yielded a significant effect of Chemo [$F(1,36) = 9.34$, $p < 0.005$, $\eta_p^2 = 0.21$], Housing effect [$F(1,36) = 9.45$, $p < 0.005$, $\eta_p^2 = 0.21$], and Chemo $\times$ Treatment Cycles interaction [$F(5,180) = 4.77$, $p < 0.0005$, $\eta_p^2 = 0.12$]. The preferential drop of BW induced by 5-FU was most convincing 24 h after completion of all five injections. Over the same period, mice receiving saline injections had essentially returned to, and indeed superseded, their baseline BW prior to the start of the first injection of each cycle (Fig. 2B). An ANOVA of %BW 24 h after completion of each cycle that best reflected the effect of 5-FU treatment cumulative within each cycle yielded a highly significant Chemo effect

[$F(1,36) = 289.11$, $p < 0.0001$, $\eta_p^2 = 0.89$], but Housing was far from significance [$F < 1$]. There was no suggestion of a Chemo by Housing interaction, indicating that ENR housing did not modify the subchronic (within-cycle) effect of 5-FU on BW reduction.

To evaluate the long-term cumulative impact of 5-FU treatment (from the first to the last treatment cycle) on BW growth, %BW recorded 24 h <u>after</u> completion of successive cycles (i.e., on days 60, 74, 88, 102, 116, 130, when the BW effect due to saline injection was no longer apparent—see Fig. 2A and 2B) was all standardized to the pre-treatment weight recorded on day 55 (= 100 %). As depicted in Fig. 2C, 5-FU treatment clearly suppressed long-term BW growth while saline injections did not. ENR/Sal and STD/Sal groups appeared highly comparable. The 5-FU-induced suppression of BW growth was notably more severe in STD than ENR mice. By day 130 into differential housing, STD/5-FU mice were below their pre-treatment weight (recorded on day 55), and ENR/5-FU mice had achieved a marginal weight gain. ENR housing was effective in attenuating long-term cumulative impact of 5-FU treatment on BW growth over this period. A $2 \times 2 \times 6$ (Chemo $\times$ Housing $\times$ Treatment Cycles) ANOVA supported these interpretations with a significant effect of Chemo [$F(1,36) = 229.79$, $p < 0.0001$, $\eta_p^2 = 0.87$], Housing [$F(1,36) = 15.75$, $p < 0.0005$, $\eta_p^2 = 0.30$], and their interaction [$F(1,36) = 10.58$, $p < 0.005$, $\eta_p^2 = 0.23$]. Planned pairwise comparisons of the interaction confirmed that the long-term weight gain
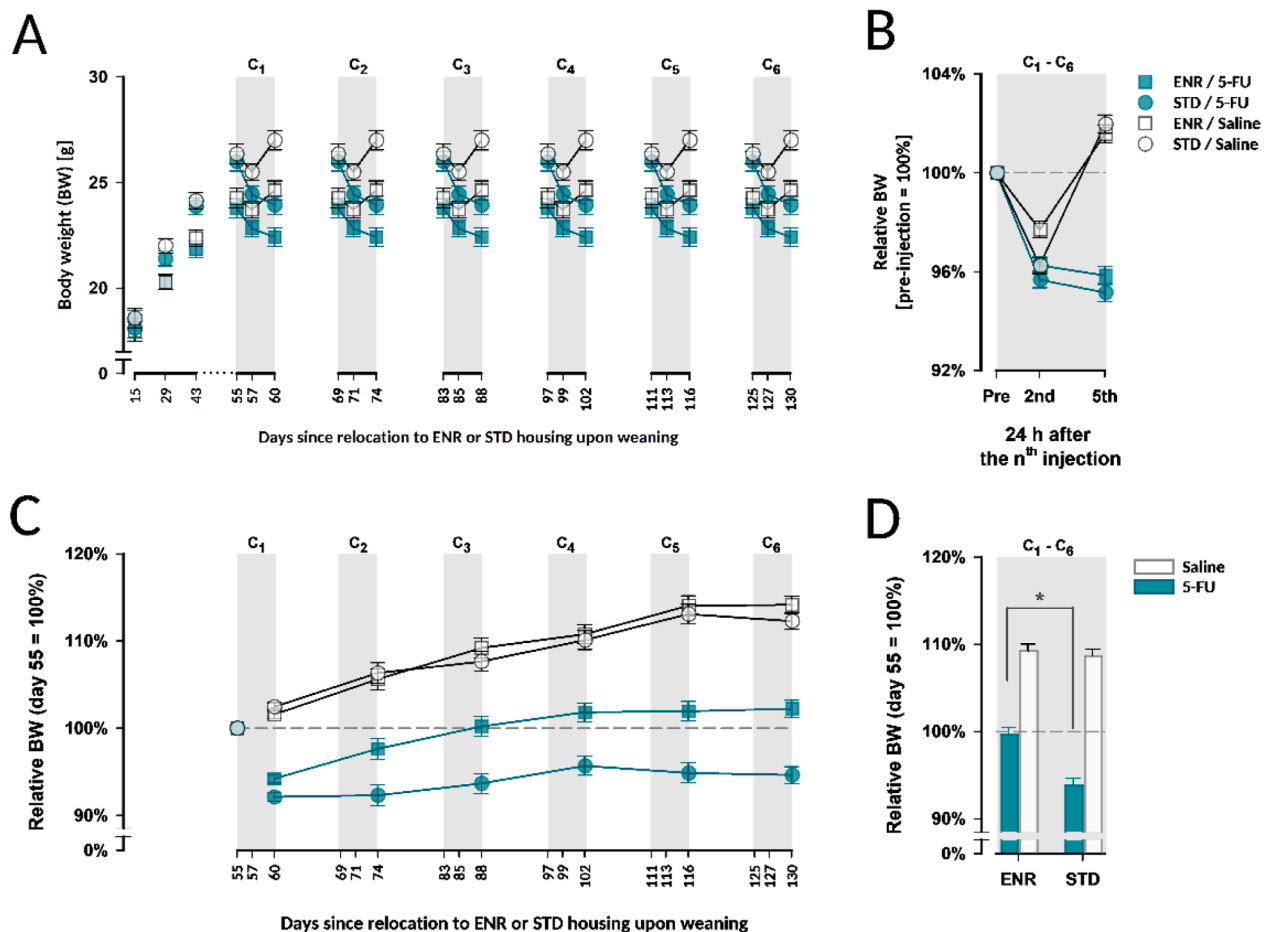

Fig. 2. Body weights (BW) over the six cycles of 5-FU treatment. **(A)** BW (in g) was recorded prior to any drug treatment (on the 15th, 29th and 43rd days since differential housing) and subsequently <u>before</u> injection on the indicated days, which spanned across the 6 treatment cycles. Successive cycles are denoted by $C_1...C_6$, with gaps in-between representing the 9-day recovery period. **(B)** The BW obtained 24 h after 2nd and 5th (=the last of a treatment cycle) injections was expressed as percentage of the BW (%BW) obtained just before the first injection of each treatment cycle (denoted as "*Pre*" = 100 %) and averaged across the 6 treatment cycles ($C_1 - C_6$). **(C)** The BW growth recorded 24 h after the last injection of each treatment cycle (days 60, 74, 88, 102, 116 and 130 since differential housing began) throughout the period is tracked as BW change (in %BW) relative to individual baseline BW recorded on day 55 (=100 %). The data are also collapsed across days and shown in **(D)**, in which "*" highlights the significant difference (Fisher's LSD, $p < 0.0001$) between 5-FU-treated ENR and STD mice. Data shown refer to mean ± standard error (SE) obtained from the SPSS output of the relevant ANOVAs. $N = 10$ per group.

over the six cycles of treatment by ENR/5-FU mice was significantly higher [$p < 0.0001$] than STD/5-FU mice who actually experienced overall weight loss (Fig. 2D). The same statistical outcomes emerged when we restricted the analysis to %BW on day 130 (Fig. 2C).

3.2. The impact of 5-FU treatment on wheel-running in ENR cages

Home cage wheel running predominantly took place in the dark phase, and this diurnal pattern was evident in both ENR cages. In the dark phase, the impact of 5-FU became apparent following the third to the fifth injection (Fig. 3A). Peak running appeared sooner after these 5-FU injections compared to saline treatment. 5-FU injections also led to more rapid fall in wheel running in the second half of the dark phase. This suppression of voluntary exercise became progressively more pronounced following the third to the fifth 5-FU injections. Both effects on home cage exercise remained apparent into the first recovery day after the last injection of the treatment cycle, but largely disappeared by the day before the next treatment cycle (i.e., on the 9th recovery day after each cycle).

Fig. 3B further illustrate the total wheel running recorded in the light or dark phase as estimated by the area under the relevant portion of the hourly curves depicted in Fig. 3A. Across the six treatment cycles, a robust reduction in voluntary running in the dark phase between the two ENR cages emerged after the fourth injection. A transient reduction in light-phase running appeared earlier after the first injection.

3.3. Behavioural profile

3.3.1. Elevated plus maze

In the maze, the mouse was free to explore two open arms, which exposed it to an unfamiliar external environment and elevation, and two enclosed arms, which were safe from such anxiety-provoking elements. Anxious mice tended to be more reluctant to venture into and explore the open arms compared to the enclosed arms, and this behaviour was taken as a proxy measure of anxiety. As illustrated in Fig. 4A-4B, 5-FU treatment intensified the expression of anxiety (i.e., anxiogenic) in mice kept in STD housing conditions only, whereas ENR-mice appeared

to be resilient to the anxiogenic effect of 5-FU.

Analysis of percent time spent, and percent entries into, the open arms (as proxy measures of anxiety, see Fig. 4A, 4B) by separate 2×2 (Chemo $\times$ Housing) ANOVAs yielded a significant interaction [% open arm time: $F_{(1,36)} = 4.86$, $p < 0.05$, $\eta_p^2 = 0.12$; % open arm entries: $F_{(1,36)} = 4.23$, $p < 0.05$, $\eta_p^2 = 0.11$]. Planned pairwise comparisons indicated that the interaction was uniquely associated with a significant difference between STD and ENR mice in the 5-FU condition [%open arm time: $p < 0.001$; % open arm entries: $p = 0.02$].

The main effect of housing was also significant [%open arm time: $F_{(1,36)} = 14.92$, $p < 0.0005$, $\eta_p^2 = 0.29$; % open arm entries: $F_{(1,36)} = 4.77$, $p < 0.05$, $\eta_p^2 = 0.29$], which essentially stemmed from the impression of an anxiolytic in 5-FU treated mice.

ENR housing also led to a concomitant increase in locomotor activity [$F_{(1,36)} = 23.73$, $p < 0.0001$, $\eta_p^2 = 0.40$]: the total distance moved on the entire maze floor was higher in ENR mice (910.91 ± 31.85 cm in 5 min) than STD mice (691.49 ± 31.85 cm). No other effect achieved statistical significance in this activity measure. Nonetheless, supplementary ANCOVAs of the two anxiety measures were performed with total distance moved as a covariate. The critical Chemo $\times$ Housing interaction remained significant [% open arm time: $F_{(1,36)} = 5.90$, $p < 0.05$, $\eta_p^2 = 0.14$; % open arms entries: $F_{(1,36)} = 5.80$, $p < 0.05$, $\eta_p^2 = 0.14$] without any diminution of this interaction's effect size in the initial ANOVAs (c.f., $\eta_p^2 = 0.12$, see preceding paragraph). Hence, the observed resilience to the 5-FU effect in ENR mice was unlikely attributable solely to the independent effects of ENR housing or 5-FU treatment on locomotor activity.

3.3.2. Open field activity

This test assessed spontaneous locomotor activity and spatial exploration over an extended area within a novel featureless and non-threatening environment. Locomotor activity and habituation were measured by the distance travelled across successive 5-min intervals (bins). 5-FU treatment was effective in suppressing locomotor activity without affecting habituation over time, but the former effect was only apparent in STD mice. Mice kept in ENR housing were notably less active than STD mice through the 30-min test and their activity profile was
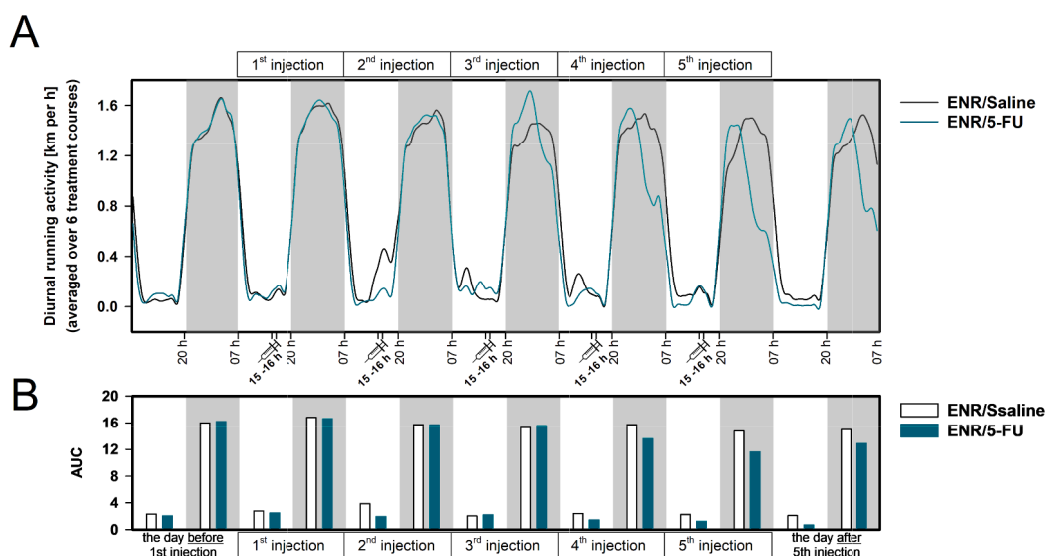

Fig. 3. The diurnal pattern of wheel-running activity average across the six cycles of treatment is compared between the ENR/Saline cage and ENR/5-FU cage. The profile in (A) depicts the hourly sum of the two running wheels (km per hour) installed in each of ENR cage (each holding 10 mice) after smoothing with 3-h running averaging. In addition to the 5 days spanning across the 5-day injection regime, the day before (baseline day) and after (recovery day) after each treatment cycle were also included. Injection was always conducted between 1500 and 1600 h as indicated. Dark phase (from 2000 to 0759 h of the following day) is highlighted by the grey background. Any short disruption of running-wheel data collection caused by cage cleaning or refreshment of enrichment items (see Fig. 1) were interpolated by corresponding hourly data from the days before and after. (B) The total distance recorded in the two cages over the light and dark phase [in km per 12 h] was estimated by the area under the curve (AUC, obtained by the trapezoidal rule) in the hourly activity curves depicted in (A).
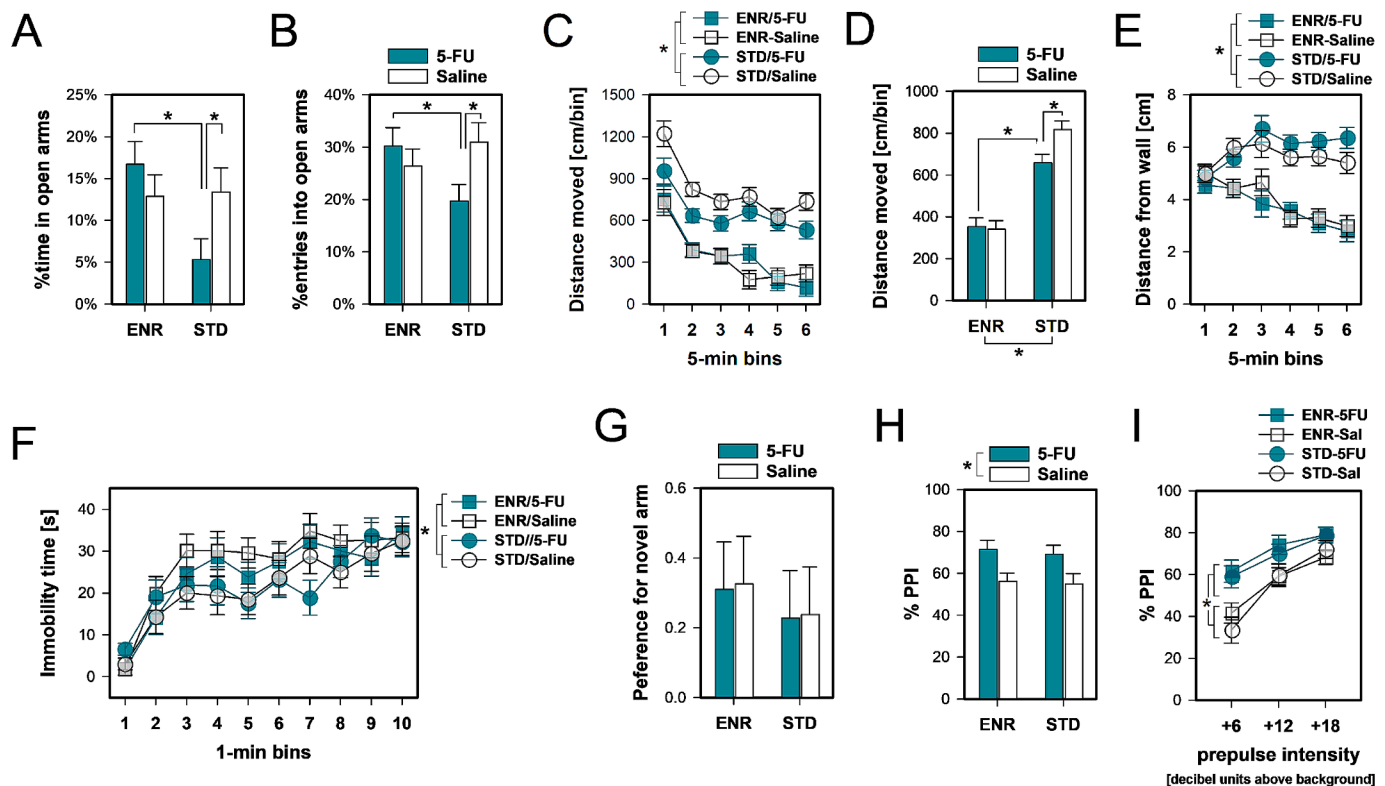
Fig. 4. Results of the behavioural tests. Anxiety-like behaviour in the elevated plus maze (EPM) test of anxiety was indexed by the relative time spent in the open arms (**A**) and relative number of entries into open arms (**B**) expressed as percent of total time spent in, and total entries into, all arms. "*" refers to significant *post hoc* pairwise that confirm the anxiogenic effect of 5-FU in STD mice, and the anxiolytic modulation by ENR housing revealed in the comparison between ENR/5-FU and STD/5-FU mice. Open field activity was indexed by distance moved across successive time bins of 5 min (5-min bins) in (**C**) or averaged over the entire 30-min observation period (**D**). The proximity to the arena wall over successive 5-min bins was indexed by the mean distance the wall per 5-min bins in (**E**). In (**C**) to (**E**), "*" in the keys or x-axis refers to the presence of a significant main effect of differential housing. Time of immobility [in sec] recorded in the Porsolt forced swim test is plotted against successive time bins of one minute (1-min bins) in (**F**), which yielded a significant main effect of differential housing (* next to keys). Performance in the Y-maze test of spatial familiarity judgement was indexed by a preference ratio (>0 indicates novelty preference, 0 = no preference) in (**G**). Prepulse inhibition was indexed by %PPI, averaged across 12 (4 levels of pulse intensity × 3 levels of prepulse intensity) conditions (**H**), and expressed as a function of increasing prepulse intensity (**I**). In (**H**) and (**I**), "*" refers to the significant main effect of Chemo emerged from the overall ANOVA. N = 10 per group in all behavioural tests. Data = mean ± SE.

largely unaffected by the 5-FU treatment (Fig. 4C, 4D).

These impressions were supported by a 2 × 2 × 6 (Chemo × Housing × Bins) ANOVA of distance moved per 5-min bin, which yielded a significant interaction between Chemo and Housing [$F(1,36) = 4.46$, $p < 0.05$, $\eta_p^2 = 0.11$], accompanied by a significant effect of Housing [$F(1,36) = 91.45$, $p < 0.0001$, $\eta_p^2 = 0.72$]. The significance of Bins [$F(5,180) = 46.02$, $p < 0.0001$, $\eta_p^2 = 0.56$] confirmed the presence of locomotor habituation, and this was similarly expressed in all four groups (Fig. 4C).

The spatial location of the mouse over the observation was tracked by its average distance from the arena walls over successive 5-min time bins. 5-FU treatment did not affect this measure, but ENR housing reduced it (Fig. 4E). All four groups remained approximately 5 cm from the arena walls over the first five minutes. Afterwards, ENR mice exhibited a progressively stronger thigmotaxis tendency down to about 3 cm to the walls, whereas STD mice explored further towards the arena centre, reaching an average distance about 6 cm from the walls by the end. The sensitivity of this measure to ENR housing led to a highly significant effect of Housing [$F(1,36) = 43.20$, $p < 0.0001$, $\eta_p^2 = 0.55$] as well as the Housing × Bins interaction [$F(5,180) = 17.97$, $p < 0.0001$, $\eta_p^2 = 0.33$], and the main effect of Bins [$F(5,180) = 7.79$, $p < 0.0001$, $\eta_p^2 = 0.18$].

3.3.3. Porsolt forced swim test

In the forced swim test, the mouse was placed in a water-filled container. After initial attempt to escape by swimming or climbing,

the animal eventually exhibited periods of immobility, which is taken as a proxy of behavioural despair or a depressive-like state. Immobility time was not significantly modified by 5-FU treatment over the 10 min test (Fig. 4G), suggesting that the chronic 5-FU was not associated with the exacerbation of behavioural despair. On the other hand, ENR housing promoted the emergence of immobility: ENR and STD mice began to diverge by the third minute-bin, but they were closely matched by the end of the test (Fig. 4F). These impressions were confirmed by a 2 × 2 × 6 (Chemo × Housing × Bins) ANOVA of immobility time that yielded a significant effect of Housing [$F(1,36) = 4.40$, $p < 0.05$, $\eta_p^2 = 0.11$], and the quadratic component of Housing × Bins interaction [$F(3,36) = 3.73$, $p < 0.05$, $\eta_p^2 = 0.24$]. The latter was consistent with differential housing affecting solely the level of immobility from bins 3 to 8 of the test. The main effect of Chemo and its interaction terms were well below statistical significance [all F's < 1] (Fig. 4G).

3.3.4. Test of spatial familiarity in the Y-maze

The test operationalizes the measurement of rodents' natural tendency to explore unfamiliar places in their environment, and thus assesses their ability to remember where they have previously been. Memories of prior visits to designated maze arms in the *sample* phase, defined solely by extra-maze landmarks, are inferred from the animal's preference for the never-visited arm when it is subsequently returned to the maze in the *test* phase.

The sample phase of the experiment was uneventful. All animals had explored the assigned arm (overall mean time ± SEM = 123.32 ± 10.66

s) and no evidence for any group differences (data not shown). In the 3-min test phase, the preferential exploration of the novel arm was not affected by the prior exposures to 5-FU. There was only a non-significant tendency of a higher preference for the novel arm in the ENR mice (Fig. 4H). A 2×2 (Chemotherapy $\times$ Housing) ANOVA on the novelty preference ratio confirmed an overall preference for the novel arm above chance [grand mean $= 0.28 \pm 0.07$, $F(1,36) = 16.68$, $p < 0.0001$, $\eta_p^2 = 0.32$]. However, it did not reveal any statistically significant effects for the main factors or their interaction [all F's < 1].

3.3.5. Prepulse inhibition of acoustic startle reflex

The test measures the whole-body motor startle reflex in response to a sudden, loud auditory burst (the pulse) and examines its reduction when preceded by a weak, non-startling stimulus (the prepulse). This reduction, known as prepulse inhibition (PPI) of the acoustic startle reflex is widely used to assess pre-attentive early sensorimotor gating.

PPI was indexed by the attenuation of startle magnitude recorded in response to the 40-ms pulse stimulus (100, 110, 115 or 120 dB) that was shortly preceded by a 20-ms prepulse (at $+ 6$, $+12$, or $+ 18$ dB units above the background noise of 65 dB) in comparison to trials in which a prepulse was not presented (i.e., $+0$ dB prepulse condition). The attenuation of the startle magnitude was expressed as percent reduction (%PPI) at each of the twelve prepulse-pulse combinations. Because differential housing and 5-FU treatment each had a notable impact on body weights (see **Section 3.1**), the body weights measured on the day of PPI were included as a covariate in all analyses in this section. The $2 \times 2 \times 4 \times 3$ (Chemo $\times$ Housing $\times$ Pulse intensity $\times$ Prepulse intensity) ANCOVA of percent %PPI showed that 5-FU treatment significantly enhanced PPI [$F(1,35) = 7.79$, $p < 0.01$, $\eta_p^2 = 0.18$] regardless of housing conditions (Fig. 4I); this was observed across all prepulse intensities but was more pronounced when the prepulse was weaker [Chemo $\times$ Prepulse intensity: $F(2,70) = 7.07$, $p < 0.005$, $\eta_p^2 = 0.17$] (Fig. 4J).

Neither 5-FU treatment nor differential housing significantly modified the startle magnitude obtained in pulse-alone trials (pulse $= 100$, 110, 115 or 120 dB). A $2 \times 2 \times 4$ (Chemo $\times$ Housing $\times$ Pulse intensity) did not yield any significant effect. 5-FU treatment also did not affect the direct response to the prepulse stimuli (including the baseline $+ 0$ dB condition), which was however sensitive to the differential housing. ENR mice showed a steeper rise in their response with increasing prepulse intensity, which yielded a significant Housing $\times$ Prepulse intensity interaction [$F(3,105) = 3.48$, $p < 0.05$, $\eta_p^2 = 0.09$] (see Supplementary Fig. 1).

Finally, habituation of the startle reflex due to repeated exposures to the startle-eliciting pulse stimuli was separately evaluated. Startle habituation was indexed by comparing the startle magnitude obtained in the first and last block of 8 pulse-alone trials by computing a suppression ratio [SR $=$ final block / (first block $+$ last block)] separately at each pulse intensity. The grand mean of SR [0.41 ± 0.02] was significantly below 0.5 [95 %CI: 0.38, 0.45], suggesting the overall presence of startle habituation. The $2 \times 2 \times 4$ (Chemo $\times$ Housing $\times$ Pulse intensity) ANCOVA of SR did not reveal any evidence for a significant Chemo or Housing effect on startle habituation.

3.4. Hippocampal immune cytokines

The six hippocampal cytokine measures were submitted to separate 2×2 (Chemo $\times$ Housing) ANOVAs after logarithmic transformation to improve the symmetry of the data distribution. 5-FU treatment only significantly elevated the level of IL-17A in the hippocampus [$F(1,36) = 5.07$, $p < 0.05$, $\eta_p^2 = 0.12$] (Fig. 5A). ENR housing appeared to exert a marginal suppression of TNFα [$F(1,36) = 3.38$, $p = 0.07$, $\eta_p^2 = 0.09$], IL17A [$F(1,36) = 3.55$, $p = 0.07$, $\eta_p^2 = 0.09$], and IL-6 [$F(1,36) = 3.44$, $p = 0.07$, $\eta_p^2 = 0.09$] of highly comparable effect size (Fig. 5B). None of the analyses yielded any suggestion for a Chemo $\times$ Housing interaction [all

F's < 1]. ENR-mice were not resistant to the IL-17A effect of 5-FU treatment, but the lower baseline IL-17 level in ENR-Sal mice might have compensated against the significant stimulatory effect of 5-FU (Fig. 5C). As a result, the levels of IL-17A between ENR/5-FU and STD/Sal appeared highly comparable.

3.5. Immature neurons in the hippocampus

3.5.1. Quantification of immature neurons labelled by DCx immunohistochemistry

As expected, ENR housing was associated with an increase in DCx-ir cells. This was more pronounced in the ventral hippocampus (by 55.02 %) than in cells sampled in the dorsal hippocampus (by 7.65 %) where DCx-ir cells were generally more abundantly observed. By contrast, the 5-FU treatment generally tended to reduce the number of DCx-ir cells. A $2 \times 2 \times 2$ (Chemo $\times$ Housing $\times$ Dorsoventral axis) ANOVA confirmed the presence of a significant Chemo [$F(1,34) = 5.22$, $p < 0.05$, $\eta_p^2 = 0.13$], Housing [$F(1,34) = 9.71$, $p < 0.005$, $\eta_p^2 = 0.22$] and Dorsoventral effect [$F(1,34) = 35.91$, $p < 0.0001$, $\eta_p^2 = 0.51$] as well as the Housing by Dorsoventral interaction [$F(1,34) = 12.27$, $p < 0.001$, $\eta_p^2 = 0.27$].

As shown in Fig. 6A, there was an impression that the 5-FU effect appeared more notable in mice kept in ENR housing compared with those in STD housing. This graphical impression was observed in both the dorsal and ventral hippocampus. However, the critical Chemo $\times$ Housing interaction did not achieve statistical significance [$F(1,34) = 2.67$, $p = 0.11$, $\eta_p^2 = 0.07$]. Nonetheless, planned pairwise comparisons confirmed that the 5-FU treatment significantly lowered the density of DCx-ir cells in ENR mice [$p = 0.035$] but not in STD mice [$p = 0.970$]. Moreover, the ENR-Saline group had the highest number of DCx-ir cells—significantly above the other three groups [all p's < 0.05]. Photomicrographs of DCx-ir cells in the dentate gyrus of sections obtained from the four groups (Std/Saline, Std/5-FU, ENR/Saline, and ENR/5-FU) are shown in Fig. 6B to 6E, respectively.

3.5.2. Sholl analysis of DCx-ir cells

There was evidence that the 5-FU treatment further reduced the arborisation of DCx-ir cells. A $2 \times 2 \times 15 \times 2$ (Chemo $\times$ Housing $\times$ Radii $\times$ Dorsoventral axis) ANOVA of the number of interactions at successive 10-μm increment from the soma obtained by Sholl analysis of DCx-ir cells sampled from the dorsal and ventral hippocampus revealed a significant effect of Chemo [$F(1,34) = 4.63$, $p < 0.05$, $\eta_p^2 = 0.12$]. The reduction further depended on Housing, Radii (i.e., distance from the soma), and the Dorsoventral axis. As depicted in Fig. 7A, the reduction emerged approximately between 70–130 μm from the soma in ENR mice, whereas the reduction appeared more subtle and restricted to a narrower band between 40–60 μm from the soma. This led to the emergence of a Chemo $\times$ Housing $\times$ Radii interaction [$F(14,476) = 2.22$, $p < 0.01$, $\eta_p^2 = 0.06$]. At the same time, modification of the 5-FU treatment effect by housing also differed between the dorsal and ventral hippocampus as suggested by the significant Chemo $\times$ Housing $\times$ Dorsoventral interaction [$F(1,34) = 4.60$, $p < 0.05$, $\eta_p^2 = 0.12$]. In the dorsal hippocampus, 5-FU treatment exerted a limited effect in the STD mice but led to a clear reduction in ENR mice (see Fig. 7D).

Evidence that the interaction between 5-FU treatment and housing conditions critically depended on the other two (within-subject) factors is confirmed by the significant 4-way interaction [$F(14,476) = 2.18$, $p < 0.01$, $\eta_p^2 = 0.06$] (Fig. 7C). Supplementary $2 \times 2 \times 15$ (Chemo $\times$ Housing $\times$ Radii) ANOVAs restricted to either the dorsal or ventral hippocampus revealed the presence of a significant Chemo $\times$ Housing interaction [$F(1,34) = 5.20$, $p < 0.05$, $\eta_p^2 = 0.13$] (Fig. 7D, dPHC plot) as well as the 3-way interaction [$F(14,476) = 2.22$, $p < 0.01$, $\eta_p^2 = 0.06$] (Fig. 7C, dPHC plot) only in the dorsal hippocampus. Neither of these effects approached statistical significance in the ANOVA restricted to the ventral hippocampus while the Chemo effect remained significant [F
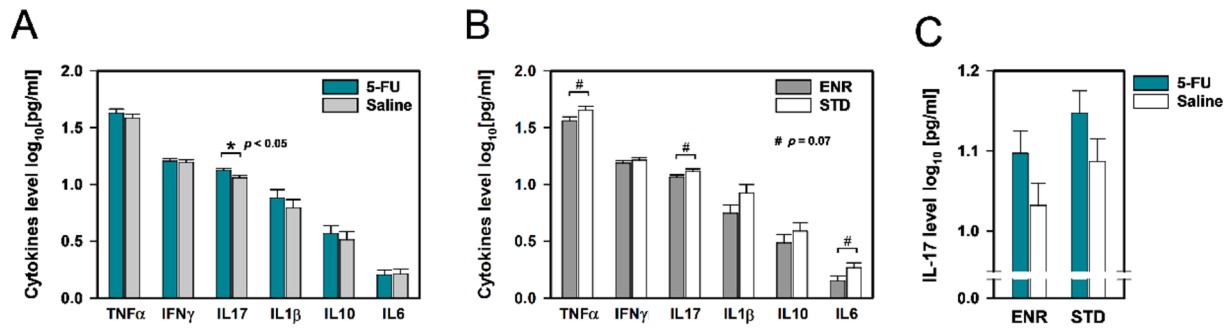
Fig. 5. Levels of immune cytokines in the hippocampus. The influence of 5-FU treatment (**A**) and differential housing (**B**) was separately presented. "*" refers to significant difference at $p < 0.05$, "#" refers to non-significant, marginal effect at $p = 0.07$. The increase in IL-17 expression caused by the 5-FU treatment is discernible in mice kept in both housing conditions, but ENR/5-FU and STD/5-FU mice appeared comparable (**C**). The logarithmic transformation was $[f(x) = \log_{10}(x + 1)]$. $N = 10$ per group. Data $=$ mean $\pm$ SE.
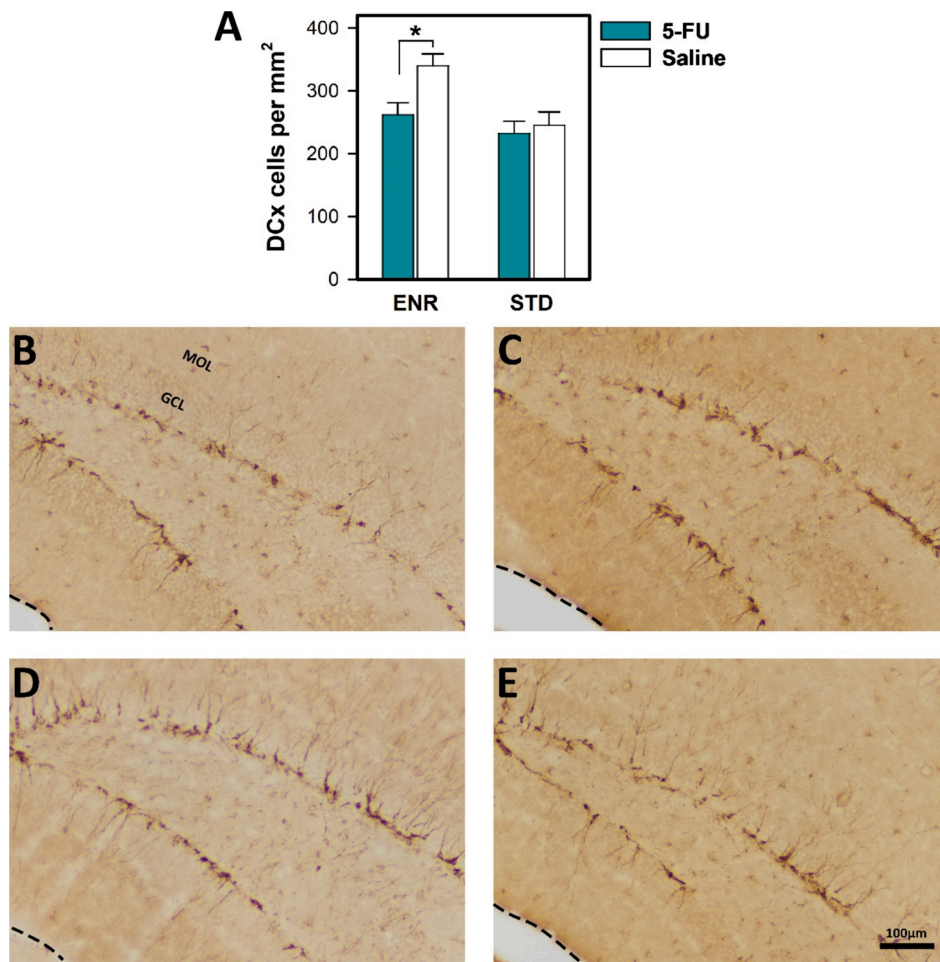
Fig. 6. (A) The mean density (cells/mm^2) of DCx-ir cells in the dentate gyrus, averaged across dorsal and ventral sections. "*" indicates that ENR/Saline group significantly differed from the rest [$p < 0.05$]. The number of mice in the STD/Saline group was reduced from 10 to 8 due to damage during histological processing. Sample size of the other groups $= 10$. Data $=$ mean $\pm$ SE. **(B–E)** Photomicrographs of DCx-ir cells in the dentate gyrus. Examples from mice from the four treatment conditions: **(B)** Std/Saline, **(C)** Std/5-FU, **(D)** ENR/Saline, and **(E)** ENR/5-FU mice. DCx-ir cells were visible in the granule cell layer (GCL), with dendritic fibers extending towards the molecular layer (MOL) and away from the hilus. Dotted lines indicate hippocampal boundaries. Scale bar $= 100$ μm.

$(1,34) = 4.66$, $p < 0.05$, $\eta_p^2 = 0.12$]. The complex dependency on the dorsoventral axis reduced the power to detect a Chemo $\times$ Housing interaction in the overall ANOVA [$F(1,34) = 1.03$, $p = 0.32$, $\eta_p^2 = 0.03$] (see Fig. 7B). In keeping with the DCx-cell count data, ENR housing appeared to enhance the sensitivity to 5-FU treatment.

3.6. Microglia in the hippocampus

3.6.1. Quantification of microglia

The 5-FU treatment led to a significant increase in the density of microglia identified by IBA1 immunostaining in the hippocampus (including CA1–CA3 and dentate gyrus). However, the increase was solely observed in mice in STD and was absent in ENR mice (Fig. 8A).
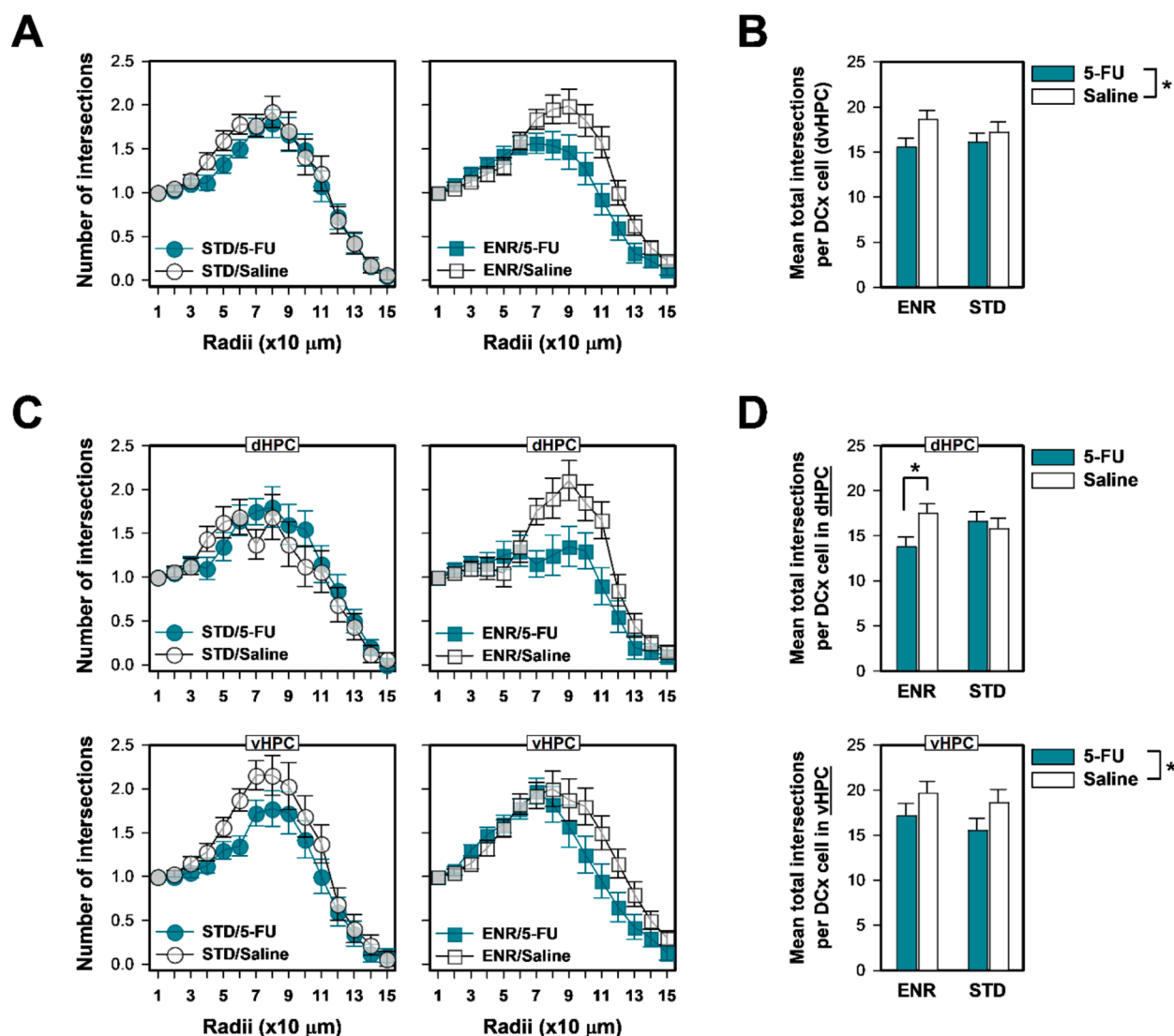
Fig. 7. Arbour complexity of neuronal processes of DCx-ir cells randomly sampled from the dorsal and ventral hippocampus was evaluated by Sholl analysis which quantified the number of intersections at successively (10 μm) increasing distance (Radii) from the cell soma (**A**). A comparison of the mean total number of intersections per cell is also provided (**B**). The respective data derived from the dorsal and ventral were also separately depicted (**C** and **D**, respectively). There is evidence that the 5-FU effect was modified by ENR housing as evident by the emergence of high-order interactions. The significant Chemo × Housing × Radii interaction, and the Chemo and Housing × Dorsoventral axis interaction, are illustrated by (**A**) and (**D**), respectively; and the significant 4-way interaction is illustrated by the set of graphs under (**C**). The Chemo × Housing interaction emerged in the ANOVA restricted to the dorsal hippocampus can be examined in the upper plot of (**D**), in which "*" refers to the significance difference between ENR/5-FU vs ENR/Saline group ($p < 0.05$). *N* per group = 8 (STD/Saline) or 10 (other groups). Data = mean ± SE.

The number of IBA1 positive cells in the hippocampus was submitted to a 2 × 2 × 2 (Chemo × Housing × Dorsoventral axis) ANOVA. Both the main effect of Chemo [$F(1,34) = 6.00$, $p < 0.05$, $\eta_p^2 = 0.15$] and the Chemo × Housing interaction [$F(1,34) = 5.58$, $p < 0.05$, $\eta_p^2 = 0.14$] achieved statistical significance. The increase in microglia density in STD mice was confirmed by planned pairwise comparison [$p = 0.01$]. By contrast, ENR mice were apparently resistant to 5-FU-induced proliferation of microglia cells in the hippocampus. Photomicrographs illustrating IBA1-ir cells in sections obtained from four individual groups (Std/Saline, Std/5-FU, ENR/Saline, and ENR/5-FU) are shown in Fig. 8D-8G.

3.6.2. Morphometric analysis of hippocampal IBA1-ir cells

The 5-FU treatment also led to an increase in average process length of IBA1-ir cells in the hippocampus, but the effect was only seen in STD mice. Although ENR mice appeared resistant to 5-FU treatment in this measure, ENR housing was associated with an increase in process length, as evident in the comparison between saline-treated ENR and STD mice (Fig. 8B). These impressions were confirmed by a 2 × 2 × 2 (Chemo × Housing × Dorsoventral axis) ANOVA, in which the between-subject factors, Chemo [$F(1,34) = 14.96$, $p < 0.0005$, $\eta_p^2 = 0.31$], Housing [$F(1,34) = 23.88$, $p < 0.0001$, $\eta_p^2 = 0.41$] as well as their interaction [$F(1,34) = 9.54$, $p < 0.005$, $\eta_p^2 = 0.22$] all achieved statistical significance. *Post hoc* comparisons indicated that STD/Sal had a significantly shorter average process length than the other three groups. The above pattern of results was consistently observed in both the dorsal and ventral levels of the hippocampus (data not shown).

A separate analysis of the mean number of endpoints per cell also revealed a significant Chemo × Housing interaction [$F(1,34) = 5.10$, $p < 0.05$, $\eta_p^2 = 0.13$], which apparently stemmed from the opposing response to 5-FU treatment differed between the two housing conditions (Fig. 8C). Neither the main effect of Chemo nor Housing achieved statistical significance [minimal $p = 0.22$]. The bidirectional response that underlined this cross interaction was associated with increased
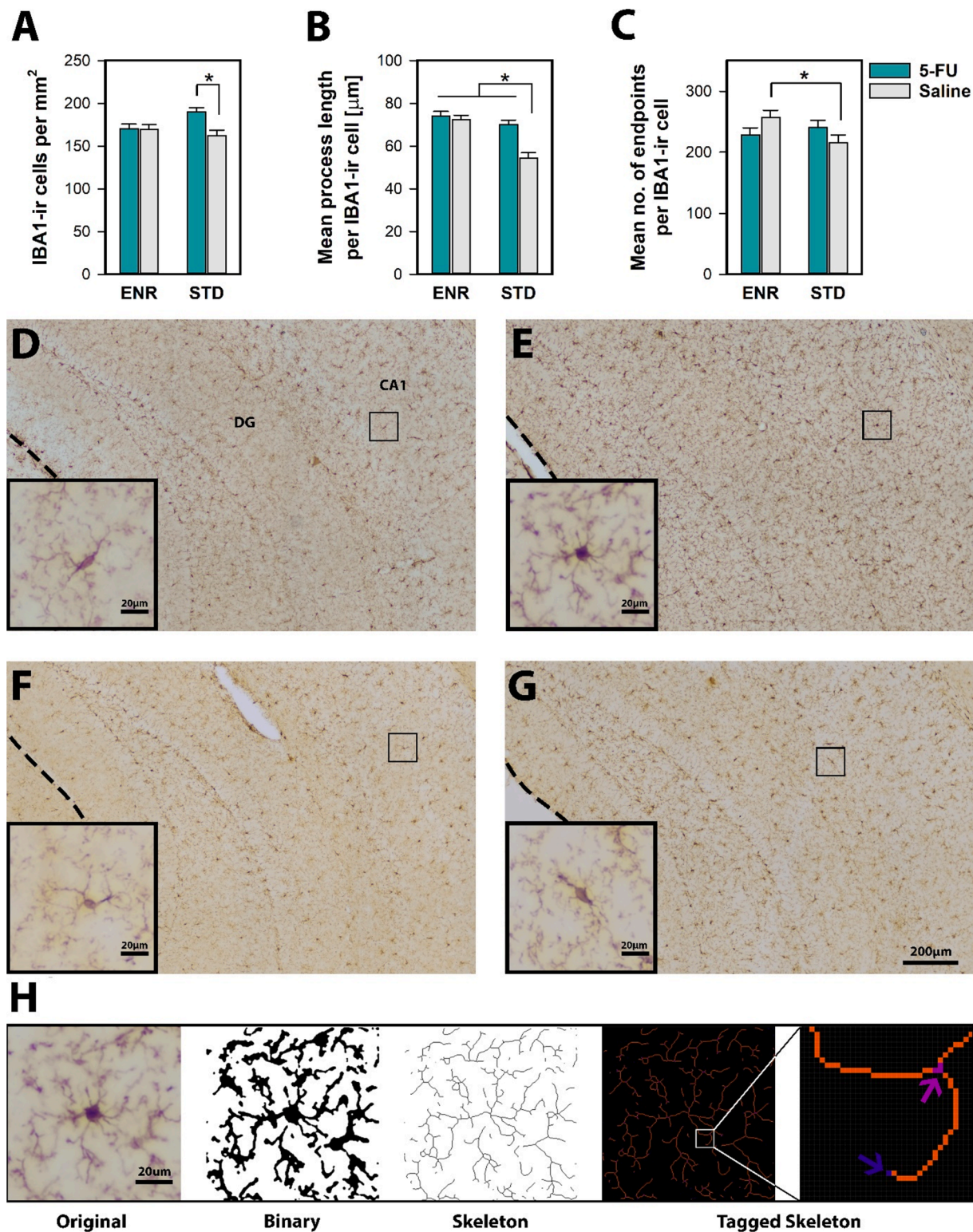
Fig. 8. Characterization of IBA1-ir microglia. The estimated number (areal density) of microglia in the hippocampus identified by IBA1 immunohistochemistry is shown in (A). Mean process length derived from the morphometric evaluation by skeletal analysis is presented in (B): The 5-FU effect was again apparent in STD but not ENR mice. Mean number of endpoints recorded per cell (C) shows a cross interaction suggesting bidirectional response to 5-FU between ENR and STD mice. All three measures yielded a significant Chemo × Housing interaction in the respective ANOVA. $N = 8$ (STD/Saline) or 10 per group. Data = mean ± SE. * indicates the significant difference between groups [$p < 0.05$] (D–G) Photomicrographs of IBA1-ir cells in the hippocampus (3.4 ~ 3.8 mm posterior to bregma). Examples from mice from the four treatment conditions: (D) Std/Saline, (E) Std/5-FU, (F) ENR/Saline, and (G) ENR/5-FU. Dotted lines indicate hippocampal boundaries. Scale bar = 100 μm. DG, dentate gyrus; CA1. One IBA1-ir cell was cropped from each image and enlarged to show in a greater magnification (Scale bar = 20 μm). The cropped IBA1-ir cell in (E) is also shown in (H) to illustrate the skeleton analysis procedure applied to this cell. From left to right, the original photomicrograph was converted to binary image after image pre-processing, which was further processed to generate the skeleton image. This skeleton image was then analysed to identify and tag the processes (orange), endpoints (blue), and junctions (purple), as shown in the two tagged skeleton images (also see Section 2.9.1). (For interpretation of the references to colour in this figure legend, the reader is referred to the web version of this article.)

microglia endpoints in ENR mice relative to STD mice in the saline condition [$p = 0.02$]. By contrast, ENR mice and STD mice exposed to 5-FU were comparable. The results were essentially independent of dorsoventral levels (data not shown).

3.7. Muscles

Each of the three muscles examined was associated with a unique pattern of response to housing and drug treatment (Fig. 9A). Separate ANOVAs revealed 5-FU treatment significantly reduced tibilias anterior (TA) mass [$F_{(1,34)} = 8.46\, p < 0.01$, $\eta_p^2 = 0.20$] whereas ENR housing led to an increase in soleus mass [$F_{(1,34)} = 16.41$, $p < 0.0005$, $\eta_p^2 = 0.33$]. Parallel analysis of TA mass expressed as percent body weight (%BW) did not yield a main effect 5-FU treatment, suggesting that the loss of TA mass could be attributed to the negative impact of 5-FU on whole body weight. On the other hand, the increase in soleus mass by ENR housing was not explicable by opposite effect of ENR housing on body weight (see Section 3.1). The independence of the differential housing effect on soleus mass was also confirmed by an ANOCVA that controlled for individual BW recorded immediately before tissue harvesting as a covariate [$F_{(1,33)} = 24.21\, p < 0.0001$, $\eta_p^2 = 0.42$]. Furthermore, soleus mass and body weight did not correlate [$r = 0.15$, $df = 36$, p = 0.15], whereas TA mass and body weight showed a strong correlation [$r = 0.75$, $df = 36$, $p < 0.0001$, $R^2 = 0.56$]. Finally, the mass of extensor digitorum longus (EDL) was unique in not showing any changes in response to either 5-FU treatment or differential housing, in terms of absolute mass or proportion of body weight [$F's < 1$].

Next, morphometric analysis of muscle fibres to isolate changes in soleus mass as its response to differential housing did not simply reflect the same effect on whole body weight. The cross-sectional counts of all fibres in the soleus taken from three randomly selected mice per condition did not reveal any significant change. Separate analyses of myofibre types, however, revealed an increase in the proportion of type 1

fibres in 5-FU treated relative to saline-treated mice regardless of housing conditions [$F_{(1,8)} = 14.82$, $p < 0.005$, $\eta_p^2 = 0.65$; 5-FU = 41.16 % vs Sal = 32.66 %, SE = 1.56 %] (Fig. 9A). Analysis of the number of type-1 fibres yielded the same impression [$F_{(1,8)} = 5.04$, $p = 0.05$, $\eta_p^2 = 0.39$; 5-FU = 317.7 vs Sal = 253.3, SE = 20.3]. Analyses of other myofibre types yielded no significant group differences.

The increase in type-1 fibre proportion in soleus was accompanied by a reduction of the size of individual type-1 muscle fibres. The 5-FU treatment led to a 11.1 % (from 34.58 to 30.74 μm) reduction in the median minimal Feret diameter [$F_{(1,8)} = 5.53$, $p < 0.05$, $\eta_p^2 = 0.41$]. No parallel change was evident in type 2A or unstained (others) fibres. Type 2B and hybrid fibres were rarely observed for meaningful statistical evaluation. Next, examination of the size distribution of type-1 fibres revealed that the 5-FU treatment shifted the distribution of type-1 fibres' Feret diameters to the left (lower sizes) but only marginally increased the spread of the distribution in the STD mice (Fig. 9C). These observations led to the emergence of a significant 3-way interaction [$F_{(9,72)} = 2.10$, $p < 0.05$, $\eta_p^2 = 0.21$] and the Chemo × Feret diameters interaction [$F_{(9,72)} = 2.99$, $p < 0.005$, $\eta_p^2 = 0.27$]. As illustrated in Fig. 9D, the 5-FU effect unique to ENR mice, whereby 5-FU led to a shift towards smaller Feret diameters resulting in a distribution comparable to STD/Sal and STD/5-FU mice (which did not differ).

3.8. Microarchitectures and mechanical properties of the femur

5-FU treatment led to a 9—10 % reduction in all three microarchitectural measures of the femur (Fig. 10). Separate 2 × 2 (Chemo × Housing) ANOVAs confirmed the presence of a significant Chemo effect [BMD: $F_{(1,32)} = 19.85$, $p < 0.0001$, $\eta_p^2 = 0.38$; BV: $F_{(1,32)} = 15.54$, $p < 0.0001$, $\eta_p^2 = 0.33$; BV/TV ratio: $F_{(1,32)} = 25.46$, $p < 0.0001$, $\eta_p^2 = 0.44$] (Fig. 10A to Fig. 10C). Enriched housing only significantly elevated BMD [$F_{(1,32)} = 4.95$, $p < 0.05$, $\eta_p^2 = 0.13$] but not any other measures. There was no evidence for an interaction between 5-FU treatment and housing
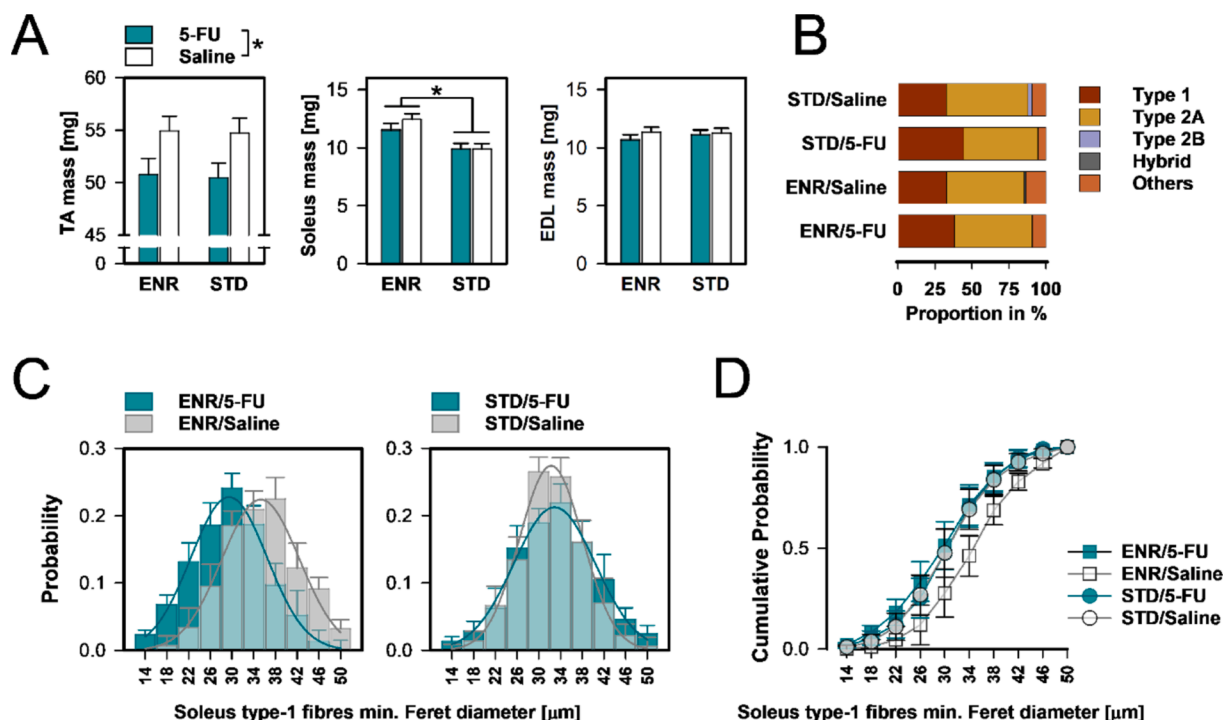

Fig. 9. Changes in muscle mass, the proportion of muscle types and fibre size distribution. (A) The mass of three separate hindlimb muscles showed differential response to the 5-FU treatment and differentially housing. **(B)** The 5-FU treatment also significantly increased the proportion of type 1 muscle fibres in the soleus. **(C)** The size distribution of soleus type-1 fibres according to individual fibres' minimal Ferret diameter was normalized and expressed as probability density. The effect of 5-FU is depicted separately for ENR mice and STD mice, and **(D)** the comparison across all four conditions is illustrated in the cumulative probability. *N* = 3 per group. Data = mean ± SE.
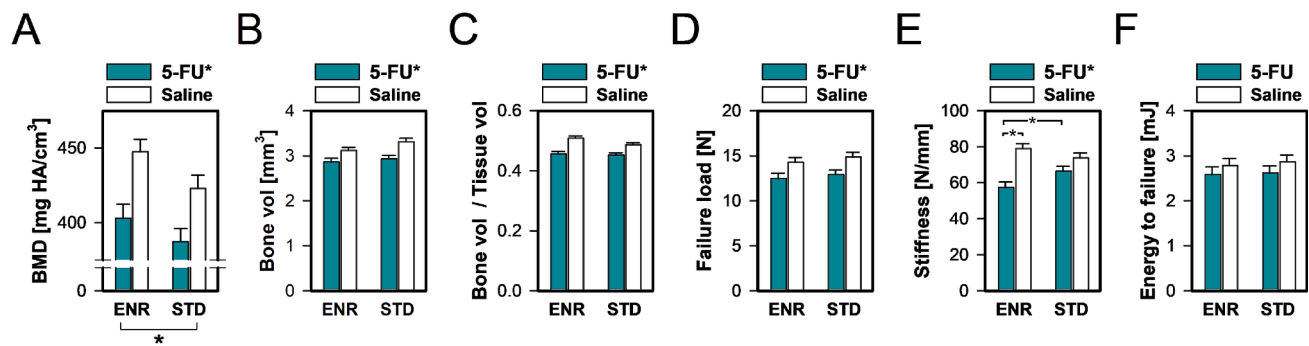
Fig. 10. Biomechanical indices obtained from the animals' left femur. BMD: Bone mineral density (**A**), bone volume (**B**), bone volume to tissue volume ratio (**C**), failure load (**D**), stiffness (**E**), and energy to failure (**F**). The integrity of the femur in two ENR/5-FU mice was compromised during harvesting ($N = 8$). The CT derived data (**A** to **C**) of the femur from one STD/Saline + one STD/5-FU were dropped due to poor image quality ($N = 9$). Otherwise, the sample size remained 10. "5-FU*" denotes the presence of a significant main effect of Chemo in the overall ANOVA of the respective variables. Data = mean ± SE.

conditions. The mechanical strength of the femur was similarly weakened by the 5-FU treatment. The reduction attained statistical significance in terms of failure load [1.49 % reduction: $F(1,34) = 11.48$, $p < 0.005$, $\eta_p^2 = 0.25$] (Fig. 10D) and stiffness [2.35 % reduction: $F(1,34) = 25.06$, $p < 0.0001$, $\eta_p^2 = 0.42$] (Fig. 10E), but not the total energy absorbed at fracture point [0.87 % reduction] (Fig. 10F). However, the reduction in stiffness due to 5-FU treatment was notably larger in mice maintained under ENR housing, leading to the emergence of the significant Chemo × Housing interaction [$F(1,34) = 6.06$, $p < 0.05$, $\eta_p^2 = 0.15$]. Post-hoc comparisons showed that the 27.4 % reduction in stiffness due to 5-FU treatment observed in the ENR mice was highly significant [$p < 0.0001$] but the 10 % reduction in stiffness observed in STD/5-FU relative to STD/Sal mice was not (Fig. 10E). Moreover, there was evidence that 5-FU lowered bone stiffness in ENR mice to a level below that in STD/5-FU group [$p < 0.05$].

4. Discussion

This study demonstrated how early sustained environmental enrichment modified the behavioural, brain and musculoskeletal responses to chronic 5-FU exposure in mice. These findings provided compelling evidence of resilience, as the anxiogenic effects and microglial proliferation seen in STD mice were nullified in ENR housing conditions. They suggested that the additional non-social elements of the ENR environment, beyond social enrichment *per se* (Walker II et al., 2020), conferred protective effects against certain adverse consequences of chronic chemotherapy exposure.

However, our model could not decide whether the ENR condition could attenuate chemotherapy-induced depression-like behaviour, as there was no evidence that our 5-FU regime had affected behaviour in the forced swim test (Fig. 4G). This lack of effect may be due to differences in chemotherapeutic drugs, or the strain and sex of mice between this study and Walker II et al. (2020). In particular, our decision to study male rather than female mice has limited direct comparison with Walker II et al. (2020), especially regarding the hypothesized role of oxytocin-mediated social interaction in females. A follow-up investigation in female mice would be warranted to explore sex-related physiological and hormonal differences, including oxytocin-dependent regulation of anxiety behaviour (see, Li et al., 2016) and sexual dimorphic effect of environmental enrichment (Wood et al., 2010). In addition, the contribution of ovariectomy performed by Walker et al. (2020) in their study also warrant further investigation, as it is not routinely performed in similar experiments (cf., Winocur et al., 2016). The interplay between female hormones and oxytocin is well known (Quintana et al., 2024), and it was suggested that ovariectomy could disrupt the modulation of oxytocin gene expression by chronic mild stress (Karisetty et al., 2017). Dissecting the contribution of ovariectomy is also relevant to our suspicion (see Introduction) that the isolation housing introduced by

Walker II et al.'s (2020) could act as an environmental stressor that had crucially contributed to the emergence of depression-like behaviour following treatment of their chosen chemotherapeutic drugs. If so, the lack of chemotherapy-induced depression-like behaviour in our study may not be surprising, because all our mice were maintained in grouped housing throughout, masking any potential antidepressant-like effects of the ENR environment.

In the present study, while some patterns of differential susceptibility to 5-FU effects between ENR and STD mice suggested that ENR housing could lead to resilience, other patterns of Housing × Chemo interaction could be interpreted differently. Specifically, there were instances where the detrimental impact of 5-FU was primarily observed in ENR mice but not in STD mice. For example, the suppression of hippocampal neural proliferation by 5-FU appeared unique to ENR mice, although this was accompanied by a baseline elevation of neural proliferation (DCx-positive cell density) in ENR/Sal mice compared to STD/Sal mice (Fig. 6A). Similar patterns were observed in the Scholl analysis of DCx-positive cells in the dorsal hippocampus (Fig. 7D), soleus fibre diameters (Fig. 9C), and bone stiffness (Fig. 10E). Among these, only bone stiffness showed a worse outcome in ENR/5-FU mice than STD/5-FU mice, suggesting a possible exacerbation by ENR housing. However, the instances did not support such a strong interpretation. Instead, they led us to speculate that the beneficial effects of ENR housing might partially underlie the apparent sensitization observed, even when the advantage of ENR/Sal mice over STD/Sal mice was not substantial. This raises the possibility that environmental enrichment could be a double-edged sword, such that our ENR mice were more vulnerable (more likely) to experience a negative change in response to 5-FU. This inference can only be directly tested in a within-subject pre-post comparison.

4.1. Improved recovery from chemotherapy-induced weight loss in the leaner ENR mice

The impact of 5-FU on physical fitness was readily demonstrated in body weight reduction. The effect appeared after the first treatment cycle and persisted (Fig. 2). Mice kept in ENR housing were not immune to this effect. However, ENR/5-FU mice gradually developed a tolerance with their body weight returning to the pre-treatment level by the third treatment cycle and even further gain in subsequent cycles. By contrast, STD/5-FU mice stabilised at 95 % of their pre-treatment weight till the end of the experiment. This magnitude of weight reduction was comparable to that reported following a subchronic regime at 50 mg/kg × 8 days (Zhang et al., 2018), which was slightly above our daily dose of 40 mg/kg. The divergent adaptation to the weight reducing effect of 5-FU between our ENR and STD mice is consistent with the suggestion that obesity could enhance susceptibility to 5FU-induced cytotoxicity (VanderVeen et al., 2022b). Being consistently leaner than STD mice, our ENR mice could be more resistant to the metabolic effects of 5-FU

(McMurphy et al., 2018; Queen et al., 2020) even though our STD mice were not excessively obese.

An effect of 5-FU on home cage voluntary wheel-running was also evident (Fig. 3). Running in the dark phase surprisingly peaked earlier in the ENR/5-FU cage. The decline also emerged sooner leading to an overall reduction in running distance. This was not only evident in the active dark phase but also apparent in the light phase. Similar reduction in home cage running was observed different schedules of 5-FU treatment: three weekly injections at 60 mg/kg (Parment et al., 2022) or 3 consecutive daily injection at 50 mg/kg (Wolff et al., 2022). Across the six treatment cycles, we also observed that the impact on wheel-running in the dark phase did not emerge until the third 5-FU injection. The effects persisted and became more pronounced after the subsequent injections and remained visible 24 h afterwards. Unlike Wolff et al. (2022) who reported suppression of home cage running lasting up two weeks before dissipating, our ENR mice fully recovered by the end of the 9-day recovery period. This matched closely with the recovery time by Mahoney et al. (2013) after treatment of 5-FU at 20–40 mg/kg, with more persistent effect only evident at 60 mg/kg in mice kept in isolation housing. Similar physical fatigue was expected to affect our mice in STD housing, but we could not evaluate if they were more severely affected. To achieve that, a more comprehensive evaluation of home cage activity by metabolic cages would be necessary, which can additionally monitor food and water intake.

4.2. The anxiogenic and motor suppressing effects of 5-FU were blocked by ENR housing

The behavioural impact of our chronic 5-FU on affective behaviour and cognitive function was evaluated after the fifth and sixth treatment cycles, respectively. Our mouse model failed to exhibit depression-like disturbance or cognitive impairments implicated in chemobrain syndrome observed in people having undergone chemotherapy. The lack of a 5-FU effect in the forced swim test, however, was consistent with two priori mouse models of 5-FU monotherapy with treatment lasting 3 to 5 weeks (37.5 to 60 mg/kg per week; Dubois et al., 2014; Parment et al., 2022). On the other hand, the absence of a deficit in the hippocampus-dependent spatial familiarity test in the Y-maze was surprising when 5-FU has been shown to impair learning in the water maze (Dubois et al., 2014; Parment et al., 2022; Elbeltagy et al., 2010). However, reports of weak and transient 5-FU-induced water maze learning deficits or null effects in other related test paradigms are not uncommon (Groves et al. 2021; Seigers et al., 2015; Fremouw et al., 2012; Lyons et al., 2012). The mixed outcomes may be related to the inconsistent effects of 5-FU suppression of hippocampal neurogenesis (see discussion below).

Nonetheless, our 5-FU treatment was far from behavioural ineffective. It selectively intensified anxiety-related behaviour, reduced locomotor activity in the open field, and potentiated the expression of sensorimotor gating.

Signs of anxiety are commonly reported in 20–30 % cancer patients (Niedzwiedz et al., 2019; Stark et al., 2002; Wittmann et al., 2006). In addition to the psychosocial perspective that emphasizes anxiety could be the coping reaction to disease burdens and concerns over treatment/ relapse (see Ahles & Saykin, 2007, Holland, 1989). Our data also agreed with previous demonstrations of an anxiogenic effect of chronic 5-FU exposure in rodents using similar ethological tests of anxiety (Parment et al. 2022, Dubois et al. 2014; Groves et al., 2021). Moreover, a similar anxiogenic effect was also reported following four weekly injections of doxorubicin (2 mg/kg/week) and cyclophosphamide (50 mg/kg/week) in rats (Kitamura et al., 2015). Hence, anxiogenesis is commonly seen side effect of chemo drugs and thus far from being unique to 5-FU (Matsos & Johnston, 2019).

Given the reliance on spontaneous explorative behaviour and movement in the EPM test of anxiety, interpretation must take into account concomitant sickness-associated behaviour such as fatigue, avolition and hypo-locomotion following 5-FU exposure, However, our EPM data were largely free from such caveats. There was essentially no group difference in total distance moved, and the selective presence of a 5-FU anxiogenic effect in the STD mice was confirmed by covariate analyses that controlled for individual differences in distance moved (Fig. 4A, 4B). It is worth noting that early life environmental enrichment was also efficacious in normalizing anxiety in the prenatal valproic acid model of autism in rats (Schneider et al., 2006). Hence, ENR housing may be associated with a general resilience against pathological anxiety beyond anxiogenesis by 5-FU. Nonetheless, the generalizability of our novel observation of resilience against 5-FU-induced anxiogenesis in our ENR mice warrants further evaluation beyond the EPM paradigm. Even though the EPM is a sensitive test of anxiety-modulating manipulations (Pellow et al., 1985), other tests of ethological anxiety such as hypo-neophagia and social interaction as well as the assessment of the acquisition and expression of learned fear (e.g., Pavlovian fear conditioning and conditioned avoidance) are warranted. Any test-specific effects may potentially differentiate the relative involvement of hippocampus- and amygdala-dependent processes.

Another interaction between housing and 5-FU treatment was observed in the open field. The suppression of open field activity evident in STD mice was clearly absent in mice kept in ENR housing (Fig. 4D). Interpreting this interaction was, however, less straightforward. Unlike in the elevated plus maze (EPM), one must consider the marked difference in open field behaviour between ENR/Sal and STD/Sal mice. While hypo-locomotor effect of 5-FU was likely attributable to fatigue, we suggest that ENR mice were less motivated to explore because the open field was relatively impoverished (lacking sensory stimulation and shelters) in comparison to their home environment (cf., Varty et al., 2000). Notably, ENR mice progressively retreated closer to the walls, but STD mice exhibited an opposite trend by moving further away from the walls (Fig. 4E). The suggestion that ENR housing had potentiated fear of open spaces as an alternative explanation would directly contradict the EPM data. The effects of hypo-locomotor due to ENR housing and 5-FU were likely distinct. Hence, we are reluctant to interpret the interaction between housing and 5-FU treatment in open field activity as evidence for resilience to 5-FU-induced physical fatigue, especially when the visible impact of 5-FU on home cage wheel running is taken into account. We suspect that locomotor exploration could be suppressed by 5-FU if the test were conducted in a more stimulating environment.

The modification of sensorimotor gating by 5-FU might seem surprising given that neuropsychiatric disturbances are typically associated with PPI impairment (Kohl et al., 2013; Santos-Carrasco & De la Casa, 2023) rather than PPI enhancement (e.g., Gogos et al., 2009; Madsen et al., 2014). We do not, however, consider this drug effect of 5-FU as a gain of function. Abnormally strong PPI may arise due to excessive attention to the weak prepulse stimulus that results in the disproportionate suppression of the startle reflex elicited by the succeeding highly salient pulse stimulus (Graham, 1975; Blumenthal, 2015). Instead, the potentiation of PPI by 5-FU could be linked to the drug's ability to suppress striatal dopamine release demonstrated in a subchronic model (25 mg/kg/day, i.v., for 1 week) (Jarmolowicz et al., 2019) because systemic dopamine blockade (e.g., by haloperidol) reliably potentiates PPI especially under a hyperdopaminergic state (Swerdlow & Geyer, 1993; Swerdlow et al., 2001, 2016; Yee et al., 2004). There were reports suggesting that environmental enrichment attenuated striatal and/or cortical dopamine activities (Segovia et al., 2008; Bellés et al., 2021). However, such alternation, if present in our ENR mice, are unlikely to counteract the PPI potentiation induced by 5-FU treatment. Indeed, ENR housing had no impact on the susceptibility to the PPI-enhancing effect of 5-FU. ENR housing also showed no effect on PPI expression as previously reported (e.g., Varty et al., 2000; Schneider et al., 2006; Hoffmann et al., 2009; Burrows et al., 2015; Nozari et al., 2015). However, there are occasional reports suggesting that environmental enrichment could enhance PPI (Chen et al., 2010; Zubedat et al., 2015; Santos et al., 2016) or attenuate PPI (Peña et al., 2009; Emack and Matthews, 2011; Hendershott et al., 2016). In such events, it remains uncertain if

environmental enrichment might exert any additive influence on the 5-FU effect.

4.3. New neurons, immune cytokines, and microglial cells in the hippocampus

The ENR housing was sufficient to stimulate the proliferation of new neurons as well as their dendritic complexity in the hippocampus (Olson et al., 2006). However, this gain in neuroplasticity was reversed by the 5-FU treatment given that ENR housing preceded well before the commencement of drug treatment. This suggests that baseline neuroplasticity could critically determine the extent to which 5-FU would reduce hippocampal neurogenesis. The progenitor cells in ENR mice's hippocampus might be more susceptible to antineoplastic effects of 5-FU because they were in a highly proliferating state compared with the STD mice. The dissimilar responses of ENR and STD mice to 5-FU could be relevant to previous divergent findings on the suppression of hippocampal neurogenesis by chronic 5-FU (Dubois et al., 2014; Mustafa et al., 2008). This impression, however, may be specifically relevant to repeated exposures to relatively low-doses of 5-FU (20 to 40 mg/kg per injection). At a very high dose (400 mg/kg, i.p.), a single 5-FU injection was sufficient to induce a persistent reduction of hippocampal DCx-positive cells (Subramaniam et al., 2023). With chronic exposure, one must also consider the possible development of tolerance against 5-FU toxicity, which might also underlie the apparent lack of substantial 5-FU treatment effects on immune cytokine expression in the hippocampus (Fig. 5A), except for the significant increase in IL-17A.

It has been suggested that elevation of IL-17A expression could contribute to the anxiety expression (Alves de Lima et al., 2020; Choi et al., 2022; Mamun-or-Rashid et al., 2024). Hence, one may be tempted to relate the elevation of IL-17A expression due to 5-FU to the drug's anxiogenic effect observed earlier. The pattern of IL-17A expression across the four groups did not match the changes in the anxiety expression. Specifically, ENR housing and 5-FU exerted opposite independently suppressed and stimulated IL-17A expression. ENR housing did not abolish the effect of 5-FU as it did in the EPM anxiety test. However, when the effect of ENR housing and 5-FU were combined, hippocampal IL-17A levels in the ENR/5-FU mice became nearly indistinguishable from STD/Sal mice (Fig. 5C). ENR housing had effectively buffered against the impact of 5-FU on IL-17A expression. If this buffering effect underlined the abolition of 5-FU anxiogenic effect by ENR housing, then one must assume that only the STD/5-FU had exceeded the threshold of IL-17A elevation to intensify anxiety.

Here, we may not easily pinpoint the potential links between immune cytokines and observed changes in microglial density and morphology to differential housing and 5-FU treatment. With hindsight, it could have been instructive if we had also investigated cytokine-mediated downstream events, since our 5-FU regime did not lead to substantial changes of hippocampal cytokines with the exception of IL-17A (Fig. 5B). Yet, significant alterations in the density and morphometric characteristics of IBA1-positive microglial cells were observed, including evidence for an interaction between differential housing and 5-FU treatment (Fig. 8). These changes were most likely the cumulative effects of the extensive 5-FU exposure here rather than an acute drug reaction. However, the observed proliferation of microglia in response to chronic 5-FU treatment in the STD mice was not accompanied by a shift towards an M1 phenotype, and therefore may not unequivocally indicate neuroinflammation in the hippocampus. Interestingly, the reduction in process length suggests a potential shift towards the M2 phenotype. This finding was unexpected and may be partly specific to our treatment schedule and dosage. To more precisely determine the relationship to chronic inflammatory reactions in the brain and behavioural changes, additional measures such as astrogliosis assessment, transcriptomic and proteomic analyses, flow cytometry, and electrophysiological analysis of microglial-neuronal interactions in slice preparations would be necessary. They could also help clarify some of the

inconsistencies regarding microglial response to 5-FU.

Seigers et al. (2016) did not observe any significant change in hippocampal microglial density at 3 or 16 weeks after 5-FU treatment (75 mg/kg, i.p.). Even at a substantially higher dosage (400 mg/kg, i.p.), Subramaniam et al. (2023) also concluded that the resultant increase in microglial density was transient. Following three injections of 5-FU/Leucovorin (50 mg/kg + 90 mg/kg, every 7 days), Groves et al. (2021) similarly failed to observe any change in the number or density of hippocampal microglial identified by CD68 immunostaining. The increase in microglial cells induced by the 5-FU treatment was further accompanied by an increase in the microglial process length. The hyper-ramified morphology may either indicate a surveillant phenotype or result of chronic stress (Torres-Platas et al., 2014; Vidal-Itriago et al., 2022). We suspect that the microglial ramification response by STD mice was a stress reaction to the chronic 5-FU exposure. If so, the absence of a drug response by the microglial of ENR mice would be consistent with numerous demonstrations of stress resiliency following environmental enrichment in laboratory rodents (e.g., Lehmann and Herkenham, 2011). By contrast, the increase in the baseline levels of microglial ramification attributed to ENR housing may be an indication of a quiescent phenotype—with a higher threshold of activation instead of association with behavioural impairments (Xu et al., 2016).

Regarding potential behavioural significance, it is worth noting that ENR housing nullified the change in microglial density (Fig. 8A) in a manner closely mirrored its resilience against the anxiogenic effect of 5-FU (Fig. 4A, 4B). In both cases, ENR housing had no effect in vehicle-treated mice. On the other hand, ENR housing and 5-FU shared a similar effect on microglial process length when measured relative to the STD/Sal group (Fig. 8B). This pattern resembled the asymmetric behavioural effect of 5-FU in the open field (Fig. 4D). Finally, the morphometric measure of endpoints also revealed a modification of 5-FU effect by ENR housing, and this interaction had features common to the two preceding interactive patterns (Fig. 8C).

4.4. The lack of resilience against chemotherapy-associated impairments in muscles and bones by ENR housing

Our data showed that not all hindlimb muscles responded equally to the 5-FU treatment in terms of mass loss. Only the TA showed a significant loss of mass after six 5-FU cycles (Fig. 9A). This muscle-specific response was also observed in a comparable 5-FU monotherapy model with three treatment cycles (35 mg/kg/day × 5 days per cycle, 9 recovery days between cycles) lasting over 30 days (VanderVeen et al., 2022b). In agreement with our observations, VanderVeen et al. (2022b) did not find a significant drop in the mass of the soleus or EDL. However, with a single cycle of a lower 5-FU dose, Campelj et al., (2021) found no apparent change in TA mass after a 12-day schedule (23 mg/kg × 6 injections).

While the soleus mass was not affected by the 5-FU treatment, it uniquely underwent hypertrophy as a result of ENR housing, while neither TA nor EDL mass was affected by ENR housing (Fig. 9A). A similar soleus-specific hypertrophy was reported following one month of environmental enrichment in juvenile rats (Sudo et al., 2023). Although other hindlimb muscles can also undergo hypertrophy and elevated myogenic satellite cell plasticity after enriched housing with voluntary wheel-running and ladder climbing (e.g., the flexor hallucis longus muscle, see Rostami et al., 2022, Sudo et al. (2023) suggested that the combination of running, climbing and standing encouraged by enriched cages preferentially promoted hypertrophy of soleus type-1 muscle fibres (Sudo et al., 2023).

In agreement with Sudo et al. (2023), ENR housing increased soleus type-1 myofibre size, but 5-FU exposure blocked this shift (Fig. 9D). It remains uncertain how 5-FU might lead to the blockade of soleus type-1 myofibre hypertrophy. The drug could directly interfere with the physiology of myogenesis, muscle remodelling or muscle memory (Gundersen, 2016) or indirectly by suppressing home cage physical

activity. Our data only permit us to conclude that the increase in soleus mass cannot be solely explained by an increase in type-1 fibres size, because 5-FU only blocked the latter ENR housing effect. Regardless, the results also gave the impression that the 5-FU treatment reduced the size of soleus type-1 fibres in ENR mice but not STD mice. This resembled the impression we had on the negative impact of 5-FU on hippocampal neural proliferation (Fig. 6A).

As expected, 5-FU caused significant deterioration to the micro-architecture and mechanical property of the femur (Fig. 10). These impairments are likely attributed to the increase in senescent cells associated with chemotherapy. Accumulation of senescent cells in the bone is associated with excessive osteoclast activity and disruption of normal bone remodelling, eventually leading to bone loss, higher risk of fractures, and bone pain (Yao et al., 2020; Xiao et al., 2023). ENR housing was unable to ameliorate the observed weakening of the femur. In agreement with suggestions that exercise could prevent osteocyte senescence through preserving mitochondrial function (e.g., Sherk and Rosen, 2019), femoral mineral density was higher in ENR mice but this was not sufficient to compensate for the more substantial reduction caused by 5-FU (Fig. 10A). Moreover, ENR mice appeared to suffer a more pronounced 5-FU-induced drop in bone stiffness (Fig. 10E), which arguably might suggest that ENR housing could exacerbate the delete-rious impact of 5-FU monotherapy. Such a claim, however, was not substantiated in other readouts since 5-FU did not actually cause a worse outcome in ENR than STD mice. However, such evidence does not necessarily contradict with findings of resilience following environ-mental enrichment. Vulnerability and resilience may be two sides of the same coin. The increased capacity for cellular plasticity associated with environmental enrichment may buffer or compensate against the im-pacts of 5-FU or give rise to covert reactions not otherwise observable in the absence of environmental enrichment. Environmental enrichment is known to improve the capacity for neuroplasticity in the brain, known as *meta*-plasticity (Deisseroth et al., 1995; Abraham and Bear, 1996; Abraham, 2008; Buschler and Manahan-Vaughan, 2012; Grau et al., 2014). It is conceivable that environmental enrichment may similarly modify the capacity for bone and muscles remodelling (Gundersen, 2016) as well as immune-triggered plasticity (Xiao et al., 2021; Hikosaka et al., 2022).

4.5. Social and environmental enrichment as a continuum

While our environmental manipulation did not directly contrast so-cial and asocial living conditions as Walker et al. (2020) did, our design provided an important extension of their investigation into psycholog-ical resilience against chemotherapy. Our STD housing and their social enriched environment were essentially the same; therefore, the two studies may be bridged along a continuum of increasing social richness: isolation →STD grouped →ENR grouped housing. By implication, pa-tients experiencing social isolation or living in impoverished environ-ments could be at greater risk of certain negative psychological impacts of chemotherapy. The non-social elements added in ENR cages are ex-pected to augment and elaborate social activities in the home cage (Stewart, 2016). The continuum emphasizes the contribution of increasingly complex and intense social interactions fostered by ENR housing compared to STD housing. It may accommodate other forms of social enrichment, such as the rotation or re-composition of cage mates (originally introduced as a form of chronic social stress by Schmidt et al. (2010); Sterlemann et al. (2008). Wang et al. (2024) showed that regular rotations of cage mates at juvenile age (for 7 weeks in C57BL/6 mice) could reduce anxiety, although whether it could yield functional resil-ience against chemotherapy (resembling our ENR housing) remains to be verified. The continuum of social enrichment procedures may facil-itate the identification of correlated brain markers towards a unifying account of functional resilience against chemotherapy.

4.6. Assessing the translatability of environmental and chemotherapeutic interactions in animal models

Our study, along with previous research, has demonstrated that environmental factors can alter animals' responses to chemotherapeutic agents. However, these findings may face criticism for lacking direct clinical applicability due to the omission of malignant growth in the models. This omission does not suggest that we consider the background or history of malignancy irrelevant. On the contrary, our approach typically views both environmental factors and malignancy (past or present) as concurrent moderating factors that collectively shape the overall response. We operate under the assumption that these factors can be examined independently, allowing their individual impacts to be dissected. By doing so, we aim to identify appropriate environmental interventions that could foster resilience in affected clinical populations.

In terms of translatability, although these models did not incorporate malignant growth, the findings still support the potential benefits of environmental and lifestyle adjustments for minimizing the negative effects of cytotoxic chemotherapy in cancer rehabilitation and pre-habilitation (Queen et al., 2020; Stout et al., 2021). Our emphasis on environmental and social enrichment (see also Walker et al., 2020; Winocur et al., 2016; Winocur, 2017) aligns with recent suggestions that such factors can even inhibit cancer proliferation (Cao et al., 2010; Cao and During, 2012).

Elements of enrichment featured in these models may correspond to the use of storytelling in hospitalized children with leukaemia to alle-viate the negative psychological responses to chemotherapy, including anxiety and pain, through engagement in positive social interaction and stimulation of oxytocin release (Brockington et al., 2021). The oxytocin-dependent mechanism revealed in this study was anticipated by Walker et al. (2020), although their model comparing social enrichment and isolation housing was conducted in female ovariectomized adult mice in the absence of malignant growth. Therefore, further translation of psy-chosocial interventions that encompass diverse elements of enrichment should be encouraged in other cancer populations, as prompted here and elsewhere (Winocur et al., 2016, 2017). This also illustrates the use of animal models to identify mechanistically relevant markers to assist in evaluating different enrichment strategies available (Flores-Ramos et al., 2022) for potential application in cancer patients.

Lastly, the present study has raised a possibility that has received scant discussion. If the resilience due to enrichment is attributed to building up physiological reserves to compensate for the negative im-pacts of chemotherapy (Fig. 5C), it may inadvertently increase the likelihood of experiencing a fall that would otherwise be less pro-nounced in the absence of preparatory intervention. Although the danger of this leading to an exacerbation of the 5-FU effect was only evident in bone stiffness (Fig. 10E), a significant drop in hippocampal neurogenesis (Figs. 6, 7D) and soleus fibre size (Fig. 9D) was selectively observed in ENR mice. Whether such enhanced physiological sensitivity might limit the broader application of environmental and psychosocial prehabilitation in the context of chemotherapy certainly warrants further exploration in animals. To reinforce our caution, while we observed a protective effect of ENR housing against 5-FU-induced anx-iety here, the social enrichment in Walker II et al.'s (2020) study appeared to sensitize the animals to the anxiogenic effect of chemo-therapy in the open field relative to the comparison group in isolated housing (see their Fig. 4I, *pp*. 458). Given that chemotherapy can pro-duce unwanted side effects in multiple organs and bodily systems, future clinical trials and preclinical models should include evaluation of pe-ripheral physiological, structural, and metabolic effects in addition to central effects on the brain and behaviour.

4.7. Conclusions

We demonstrated that sustained environmental enrichment from an early age can significantly alter the behavioural, immune, and

physiological responses of laboratory mice to chronic exposure to 5-FU. The most notable impact of enriched housing was the protection against 5-FU-induced anxiety, and the parallel resistance to microglial proliferation. Whether these specific concomitant impacts of enriched housing may indicate an environmental moderation of the link between brain inflammatory state and behaviour warrants further investigation. In addition, there were instances that enriched housing led to a reserve capacity that independently countered the effects of chronic 5-FU that may be described as compensatory resilience. Finally, we identified certain central as well as peripheral effects of 5-FU that were preferentially seen in mice maintained in enriched environments. These observations highlight at least some negative effects of chronic 5-FU exposure might be sensitized by environmental enrichment.

CRediT authorship contribution statement

Vic K.T. Sun: Writing – review & editing, Project administration, Methodology, Investigation, Formal analysis, Conceptualization. **Jimmy W.Y. Lam:** Writing – review & editing, Visualization, Investigation, Formal analysis, Data curation. **Marcus H.F. Ng:** Writing – review & editing, Visualization, Methodology, Investigation, Formal analysis, Data curation. **Wing-Yan Wong:** Investigation. **William C.S. Tai:** Investigation, Conceptualization. **Dick H.K. Chow:** Investigation. **Alex K.K. Cheung:** Resources, Investigation, Funding acquisition. **Benson W.M. Lau:** Writing – review & editing, Funding acquisition. **Andy S.K. Cheng:** Funding acquisition. **Benjamin K. Yee:** Writing – review & editing, Writing – original draft, Visualization, Supervision, Project administration, Methodology, Funding acquisition, Formal analysis, Conceptualization.

Declaration of Competing Interest

The authors declare that they have no known competing financial interests or personal relationships that could have appeared to influence the work reported in this paper.

Acknowledgements

Appendix A. Supplementary data

Supplementary data to this article can be found online at https://doi.org/10.1016/j.bbi.2025.01.009.

Data availability

Data will be made available on request.

References

Abraham, W.C., 2008. Metaplasticity: tuning synapses and networks for plasticity. Nat. Rev. Neurosci. 9, 387.

Abraham, W.C., Bear, M.F., 1996. Metaplasticity: the plasticity of synaptic plasticity. Trends Neurosci. 19, 126–130.

Ahles, T.A., Saykin, A.J., 2007. Candidate mechanisms for chemotherapy-induced cognitive changes. Nat. Rev. Cancer 7, 192–201.

Aires, I., Duarte, J.A., Vitorino, R., Moreira-Gonçalves, D., Oliveira, P., Ferreira, R., 2024. Restoring skeletal muscle health through exercise in breast cancer patients and after receiving chemotherapy. IJMS 25, 7533.

Alves de Lima, K., Rustenhoven, J., Da Mesquita, S., Wall, M., Salvador, A., Smirnov, I., Cebinelli, G., Mamuladze, T., Baker, W., Papadopoulos, Z., 2020. Meningeal γδ T cells regulate anxiety-like behavior via IL-17a signaling in neurons. Biol. Psychiatry 89, S65.

Bellés, L., Dimiziani, A., Herrmann, F.R., Ginovart, N., 2021. Early environmental enrichment and impoverishment differentially affect addiction-related behavioral traits, cocaine-taking, and dopamine D2/3 receptor signaling in a rat model of vulnerability to drug abuse. Psychopharmacology 238, 3543–3557.

Blumenthal, T.D., 2015. Presidential Address 2014: The more-or-less interrupting effects of the startle response. Psychophysiology 52, 1417–1431.

Bondi, C.O., Klitsch, K.C., Leary, J.B., Kline, A.E., 2014. Environmental enrichment as a viable neurorehabilitation strategy for experimental traumatic brain injury. J. Neurotrauma 31, 873–888.

Bouxsein, M.L., Boyd, S.K., Christiansen, B.A., Guldberg, R.E., Jepsen, K.J., Müller, R., 2010. Guidelines for assessment of bone microstructure in rodents using micro–computed tomography. J. Bone Miner. Res. 25, 1468–1486.

Brockington, G., Gomes Moreira, A.P., Buso, M.S., Gomes da Silva, S., Altszyler, E., Fischer, R., Moll, J., 2021. Storytelling increases oxytocin and positive emotions and decreases cortisol and pain in hospitalized children. Proc. Natl. Acad. Sci. U.S.A. 118.

Burrows, E.L., McOmish, C.E., Buret, L.S., Van den Buuse, M., Hannan, A.J., 2015. Environmental enrichment ameliorates behavioral impairments modeling schizophrenia in mice lacking metabotropic glutamate receptor 5. Neuropsychopharmacol 40, 1947–1956.

Buschler, A., Manahan-Vaughan, D., 2012. Brief environmental enrichment elicits metaplasticity of hippocampal synaptic potentiation in vivo. Front. Behav. Neurosci. 6.

Campelj, D.G., Timpani, C.A., Cree, T., Petersen, A.C., Hayes, A., Goodman, C.A., Rybalka, E., 2021. Metronomic 5-fluorouracil delivery primes skeletal muscle for myopathy but does not cause cachexia. Pharmaceuticals 14, 478.

Cao, L., During, M.J., 2012. What is the brain-cancer connection? Annu. Rev. Neurosci. 35, 331–345.

Cao, L., Liu, X., Lin, E.-J.-D., Wang, C., Choi, E.Y., Riban, V., Lin, B., During, M.J., 2010. Environmental and genetic activation of a brain-adipocyte BDNF/leptin axis causes cancer remission and inhibition. Cell 142, 52–64.

Chen, Y., Mao, Y., Zhou, D., Hu, X., Wang, J., Ma, Y., 2010. Environmental enrichment and chronic restraint stress in ICR mice: effects on prepulse inhibition of startle and Y-maze spatial recognition memory. Behav. Brain Res. 212, 49–55.

Choi, I.-Y., Cho, M.-L., Cho, K.-O., 2022. Interleukin-17A Mediates Hippocampal Damage and Aberrant Neurogenesis Contributing to Epilepsy-Associated Anxiety. Front. Mol. Neurosci. 15.

Cotman, C.W., Engesser-Cesar, C., 2002. Exercise enhances and protects brain function. Exerc. Sport Sci. Rev. 30, 75–79.

Csomor, P.A., Yee, B.K., Vollenweider, F.X., Feldon, J., Nicolet, T., Quednow, B.B., 2008. On the influence of baseline startle reactivity on the indexation of prepulse inhibition. Behav Neurosci 122 (4), 885–900.

Dantzer, R., O'Connor, J.C., Freund, G.C., Johnson, R.W., Kelley, K.W., 2008. From inflammation to sickness and depression: When the immune system subjugates the brain. Nat. Rev. Neurosci. 9, 46–57.

Deisseroth, K., Bito, H., Schulman, H., Tsien, R.W., 1995. Synaptic plasticity: a molecular mechanism for metaplasticity. Curr. Biol. 5, 1334–1338.

Diamond, M.C., 1988. Enriching heredity: The Impact of the Environment on the Anatomy of the Brain. Weidenfeld & Nicolson, New York.

Dubois, M., Lapinte, N., Villier, V., Lecointre, C., Roy, V., Tonon, M.-C., Gandolfo, P., Joly, F., Hilber, P., Castel, H., 2014. Chemotherapy-induced long-term alteration of executive functions and hippocampal cell proliferation: Role of glucose as adjuvant. Neuropharmacology 79, 234–248.

ELBeltagy, M., Mustafa, S., Umka, J., Lyons, L., Salman, A., Gloria Tu, C.-Y., Bhalla, N., Bennett, G., Wigmore, P.M., 2010. Fluoxetine improves the memory deficits caused by the chemotherapy agent 5-fluorouracil. Behav. Brain Res. 208, 112–117.

Emack, J., Matthews, S.G., 2011. Effects of chronic maternal stress on hypothalamo–pituitary–adrenal (HPA) function and behavior: No reversal by environmental enrichment. Horm. Behav. 60, 589–598.

Encarnacion-Rivera, L., Foltz, S., Hartzell, H.C., Choo, H., 2020. Myosoft: an automated muscle histology analysis tool using machine learning algorithm utilizing FIJI/ImageJ software. PLoS One 15, e0229041.

Fernandez-Teruel, A., Escorihuela, R.M., Castellano, B., González, B., Tobeña, A., 1997. Neonatal handling and environmental enrichment effects on emotionality, novelty/reward seeking, and age-related cognitive and hippocampal impairments: focus on the Roman rat lines 27, 513–526.

Flores-Ramos, M., Yoldi-Negrete, M., Guiza-Zayas, R., Ramírez-Rodríguez, G.-B., Montes-Castrejón, A., Fresán, A., 2022. An Indicator of environmental enrichment to measure physical, social and cognitive activities in human daily life. BMC Psychiatry 22.

Franklin, J.C., Bowker, K.C., Blumenthal, T.D., 2007. The association between schizoid and histrionic personality disorder traits and prepulse inhibition of acoustic startle in

a nonclincial sample. In: 47th Annual Meeting of the Society-for-Psychophysiological-Research.

Fremouw, T., Fessler, C.L., Ferguson, R.J., Burguete, Y., 2012. Preserved learning and memory in mice following chemotherapy: 5-Fluorouracil and doxorubicin single agent treatment, doxorubicin–cyclophosphamide combination treatment. Behav. Brain Res. 226, 154–162.

Gogos, A., van den Buuse, M., Rossell, S., 2009. Gender differences in prepulse inhibition (PPI) in bipolar disorder: men have reduced PPI, women have increased PPI. Int. J. Neuropsychopharm. 12, 1249.

Graham, F.K., 1975. The more or less startling effects of weak prestimulation. Psychophysiology 12, 238–248.

Grau, J.W., Huie, J.R., Lee, K.H., Hoy, K.C., Huang, Y.-J., Turtle, J.D., Strain, M.M., Baumbauer, K.M., Miranda, R.M., Hook, M.A., 2014. Metaplasticity and behavior: how training and inflammation affect plastic potential within the spinal cord and recovery after injury. Front. Neural Circuits. 8.

Groves, T., Corley, C., Byrum, S.D., Allen, A.R., 2021. The Effects of 5-Fluorouracil/Leucovorin Chemotherapy on Cognitive Function in Male Mice. Front. Mol. Biosci. 8.

Gundersen, K., 2016. Muscle memory and a new cellular model for muscle atrophy and hypertrophy 219, 235–242.

Hebb, D.O., 1947. The effects of early experience on problem-solving at maturity. Am. Psychol. 2, 737–745.

Hendershott, T.R., Cronin, M.E., Langella, S., McGuinness, P.S., Basu, A.C., 2016. Effects of environmental enrichment on anxiety-like behavior, sociability, sensory gating, and spatial learning in male and female C57BL/6J mice. Behav. Brain Res. 314, 215–225.

Hikosaka, M., Kawano, T., Wada, Y., Maeda, T., Sakurai, T., Ohtsuki, G., 2022. Immune-Triggered Forms of Plasticity Across Brain Regions. Front. Cell. Neurosci. 16.

Hoffmann, L.C., Schütte, S.R.M., Koch, M., Schwabe, K., 2009. Effect of "enriched environment" during development on adult rat behavior and response to the dopamine receptor agonist apomorphine. Neuroscience 158, 1589–1598.

Holland, J.C., 1989. Anxiety and cancer: the patient and the family. J. Clin. Psychiatry 50, 20–25.

Huang, L., Wang, X., Cao, H., Li, L., Chow, D.-H.-K., Tian, L., Wu, H., Zhang, J., Wang, N., Zheng, L., 2018. A bone-targeting delivery system carrying osteogenic phytomolecule icaritin prevents osteoporosis in mice. Biomaterials 182, 58–71.

Huang, L., You, Y., Zhu, T.Y., Zheng, L., Huang, X., Chen, H., Yao, D., Lan, H., Qin, L., 2016. Validity of leptin receptor-deficiency (db/db) type 2 diabetes mellitus mice as a model of secondary osteoporosis. Sci. Rep. 6.

Hughes, S., Jaremka, L.M., Alfano, C.M., Glaser, R., Povoski, S.P., Lipari, A.M., Agnese, D.M., Farrar, W.B., Yee, L.D., Carson, W.E., 2014. Social support predicts inflammation, pain, and depressive symptoms: longitudinal relationships among breast cancer survivors. Psychoneuroendocrinology 42, 38–44.

Isaksson, H., Tolvanen, V., Finnilä, M.A.J., Iivarinen, J., Tuukkanen, J., Seppänen, K., Arokoski, J.P.A., Brama, P.A., Jurvelin, J.S., Helminen, H.J., 2009. Physical exercise improves properties of bone and its collagen network in growing and maturing mice. Calcif. Tissue Int. 85, 247–256.

Jarmolowicz, D.P., Gehringer, R., Lemley, S.M., Sofis, M.J., Kaplan, S., Johnson, M.A., 2019. 5-Fluorouracil impairs attention and dopamine release in rats. Behav. Brain Res. 362, 319–322.

Karisetty, B.C., Khandelwal, N., Kumar, A., Chakravarty, S., 2017. Sex difference in mouse hypothalamic transcriptome profile in stress-induced depression model. Biochem. Biophys. Res. Commun. 486, 1122–1128.

Kentner, A.C., Cryan, J.F., Brummelte, S., 2019. Resilience priming: Translational models for understanding resiliency and adaptation to early life adversity. Dev. Psychobiol. 61, 350–375.

Kentner, A.C., Khoury, A., Lima Queiroz, E., MacRae, M., 2016. Environmental enrichment rescues the effects of early life inflammation on markers of synaptic transmission and plasticity. Brain Behav. Immun. 57, 151–160.

Kim, Y.J., Kim, H.J., Lee, W.J., Seong, J.K., 2020. A comparison of the metabolic effects of treadmill and wheel running exercise in mouse model. Lab Anim Res 36.

Kitamura, Y., Hattori, S., Yoneda, S., Watanabe, S., Kanemoto, E., Sugimoto, M., Kawai, T., Machida, A., Kanzaki, H., Miyazaki, I., 2015. Doxorubicin and cyclophosphamide treatment produces anxiety-like behavior and spatial cognition impairment in rats: possible involvement of hippocampal neurogenesis via brain-derived neurotrophic factor and cyclin D1 regulation. Behav. Brain Res. 292, 184–193.

Kobiec, T., Mardaraz, C., Toro-Urrego, N., Kölliker-Frers, R., Capani, F., Otero-Losada, M., 2023. Neuroprotection in metabolic syndrome by environmental enrichment. A lifespan perspective. Front. Neurosci. 17.

Kohl, S., Heekeren, K., Klosterkötter, J., Kuhn, J., 2013. Prepulse inhibition in psychiatric disorders – Apart from schizophrenia. J. Psychiatr. Res. 47, 445–452.

Lehmann, M.L., Herkenham, M., 2011. Environmental enrichment confers stress resiliency to social defeat through an infralimbic cortex-dependent neuroanatomical pathway. J. Neurosci. 31, 6159–6173.

Li, K., Nakajima, M., Ibañez-Tallon, I., Heintz, N., 2016. A cortical circuit for sexually dimorphic oxytocin-dependent anxiety behaviors. Cell 167, 60–72.

Longley, D.B., Harkin, D.P., Johnston, P.G., 2003. 5-Fluorouracil: mechanisms of action and clinical strategies. Nat. Rev. Cancer 3, 330–338.

Lyons, L., ELBeltagy, M., Bennett, G., Wigmore, P., 2012. Fluoxetine counteracts the cognitive and cellular effects of 5-fluorouracil in the rat hippocampus by a mechanism of prevention rather than recovery. PLoS One 7, e30010.

Madsen, G.F., Bilenberg, N., Cantio, C., Oranje, B., 2014. Increased prepulse inhibition and sensitization of the startle reflex in autistic children. Autism Res. 7, 94–103.

Mahoney, S.E., Davis, J.M., Murphy, E.A., McClellan, J.L., Gordon, B., Pena, M.M., 2013. Effects of 5-fluorouracil chemotherapy on fatigue: role of MCP-1. Brain Behav. Immun. 27, 155–161.

Mamun-or-Rashid, Roknuzzaman, A.S.M., Sarker, R., Nayem, J., Bhuiyan, M.A., Islam, Md.R., Al Mahmud, Z., 2024. Altered serum interleukin-17A and interleukin-23A levels may be associated with the pathophysiology and development of generalized anxiety disorder. Sci. Rep. 14.

Matsos, A., Johnston, I.N., 2019. Chemotherapy-induced cognitive impairments: a systematic review of the animal literature. Neurosci. Biobehav. Rev. 102, 382–399.

McFarlane, E., Burrell, L., Duggan, A., Tandon, S., 2017. Outcomes of a randomized trial of a cognitive behavioral enhancement to address maternal distress in home visited mothers. Matern. Child Health J. 21, 475–484.

McMurphy, T., Huang, W., Queen, N.J., Ali, S., Widstrom, K.J., Liu, X., Xiao, R., Siu, J.J., Cao, L., 2018. Implementation of environmental enrichment after middle age promotes healthy aging. Aging 10, 1698–1721.

Mustafa, S., Walker, A., Bennett, G., Wigmore, P.M., 2008. 5-Fluorouracil chemotherapy affects spatial working memory and newborn neurons in the adult rat hippocampus. Eur. J. Neurosci. 28, 323–330.

National Research Council of the National Academies (U.S.), 2011. Care and Use of Laboratory Animals, Eighth edition. ed. Washington, DC: The National Academies Press.

Niedzwiedz, C.L., Knifton, L., Robb, K.A., Katikireddi, S.V., Smith, D.J., 2019. Depression and anxiety among people living with and beyond cancer: a growing clinical and research priority. BMC Cancer 19.

Nozari, M., Shabani, M., Farhangi, A.M., Mazhari, S., Atapour, N., 2015. Sex-specific restoration of MK-801-induced sensorimotor gating deficit by environmental enrichment. Neuroscience 299, 28–34.

Olson, A.K., Eadie, B.D., Ernst, C., Christie, B.R., 2006. Environmental enrichment and voluntary exercise massively increase neurogenesis in the adult hippocampus via dissociable pathways. Hippocampus 16, 250–260.

Parment, R., Dubois, M., Desrues, L., Mutel, A., Dembélé, K.-P., Belin, N., Tron, L., Guérin, C., Coëffier, M., Compère, V., 2022. A panax quinquefolius-based preparation prevents the impact of 5-FU on activity/exploration behaviors and not on cognitive functions mitigating gut microbiota and inflammation in mice. Cancers 14, 4403.

Pellow, S., Chopin, P., File, S.E., Briley, M., 1985. Validation of open: closed arm entries in an elevated plus-maze as a measure of anxiety in the rat. J. Neurosci. Methods 14, 149–167.

Peña, Y., Prunell, M., Rotllant, D., Armario, A., Escorihuela, R.M., 2009. Enduring effects of environmental enrichment from weaning to adulthood on pituitary-adrenal function, pre-pulse inhibition and learning in male and female rats. Psychoneuroendocrinology 34, 1390–1404.

Pietropaolo, S., Feldon, J., Alleva, E., Cirulli, F., Yee, B.K., 2006. The role of voluntary exercise in enriched rearing: a behavioral analysis. Behav. Neurosci. 120, 787–803.

Pietropaolo, S., Feldon, J., Yee, B.K., 2014. Environmental enrichment eliminates the anxiety phenotypes in a triple transgenic mouse model of Alzheimer's disease. Cogn. Affect. Behav. Neurosci. 14, 996–1008.

Queen, N.J., Hassan, Q.N., Cao, L., 2020. Improvements to Healthspan Through Environmental Enrichment and Lifestyle Interventions: Where Are We Now? Front. Neurosci. 14.

Quintana, D.S., Glaser, B.D., Kang, H., Kildal, E.S.M., Audunsdottir, K., Sartorius, A.M., Barth, C., 2024. The interplay of oxytocin and sex hormones. Neurosci. Biobehav. Rev. 163, 105765.

Raine, A., Mellingen, K., Liu, J., Venables, P., Mednick, S.A., 2003. Effects of environmental enrichment at ages 3–5 years on schizotypal personality and antisocial behavior at ages 17 and 23 Years. AJP 160, 1627–1635.

Reid-Arndt, S.A., Hsieh, C., Perry, M.C., 2010. Neuropsychological functioning and quality of life during the first year after completing chemotherapy for breast cancer. Psychooncology 19, 535–544.

Renner, M.J., Rosenzweig, M.R., 1987. The golden-mantled ground squirrel (Spermophilus lateralis) as a model for the effects of environmental enrichment in solitary animals. Dev. Psychobiol. 20, 19–24.

Rostami, S., Salehizadeh, N., Shamloo, S., Fayazmilani, R., 2022. The Effect of Voluntary Physical Activity in an Enriched Environment and Combined Exercise Training on the Satellite Cell Pool in Developing Rats. Front. Physiol. 13.

Salama, J.K., Haraf, D.J., Stenson, K.M., Blair, E.A., Witt, M.E., Williams, R., Kunnavakkam, R., Cohen, E.E.W., Seiwert, T., Vokes, E.E., 2011. A randomized phase II study of 5-fluorouracil, hydroxyurea, and twice-daily radiotherapy compared with bevacizumab plus 5-fluorouracil, hydroxyurea, and twice-daily radiotherapy for intermediate-stage and T4N0-1 head and neck cancers. Ann. Oncol. 22, 2304–2309.

Santos, C.M., Peres, F.F., Diana, M.C., Justi, V., Suiama, M.A., Santana, M.G., Abílio, V. C., 2016. Peripubertal exposure to environmental enrichment prevents schizophrenia-like behaviors in the SHR strain animal model. Schizophr. Res. 176, 552–559.

Santos-Carrasco, D., De la Casa, L.G., 2023. Prepulse inhibition deficit as a transdiagnostic process in neuropsychiatric disorders: a systematic review. BMC Psychol. 11.

Schindelin, J., Arganda-Carreras, I., Frise, E., Kaynig, V., Longair, M., Pietzsch, T., Preibisch, S., Rueden, C., Saalfeld, S., Schmid, B., 2012. Fiji: an open-source platform for biological-image analysis. Nat. Methods 9, 676–682.

Schmidt, M.V., Scharf, S.H., Sterlemann, V., Ganea, K., Liebl, C., Holsboer, F., Müller, M. B., 2010. High susceptibility to chronic social stress is associated with a depression-like phenotype. Psychoneuroendocrinology 35, 635–643.

Schneider, T., Turczak, J., Przewłocki, R., 2006. Environmental enrichment reverses behavioral alterations in rats prenatally exposed to valproic acid: issues for a therapeutic approach in autism. Neuropsychopharmacol 31, 36–46.

Segovia, G., Delarco, A., Deblas, M., Garrido, P., Mora, F., 2008. Effects of an enriched environment on the release of dopamine in the prefrontal cortex produced by stress

and on working memory during aging in the awake rat. Behav. Brain Res. 187, 304–311.

Seigers, R., Loos, M., Van Tellingen, O., Boogerd, W., Smit, A.B., Schagen, S.B., 2015. Cognitive impact of cytotoxic agents in mice. Psychopharmacology 232, 17–37.

Seigers, R., Loos, M., Van Tellingen, O., Boogerd, W., Smit, A.B., Schagen, S.B., 2016. Neurobiological changes by cytotoxic agents in mice. Behav. Brain Res. 299, 19–26.

Sherk, V.D., Rosen, C.J., 2019. Senescent and apoptotic osteocytes and aging: exercise to the rescue? Bone 121, 255–258.

Sougiannis, A.T., VanderVeen, B.N., Enos, R.T., Velazquez, K.T., Bader, J.E., Carson, M., Chatzistamou, I., Walla, M., Pena, M.M., Kubinak, J.L., 2019. Impact of 5 fluorouracil chemotherapy on gut inflammation, functional parameters, and gut microbiota. Brain Behav. Immun. 80, 44–55.

Stark, D., Kiely, M., Smith, A., Velikova, G., House, A., Selby, P., 2002. Anxiety disorders in cancer patients: their nature, associations, and relation to quality of life. J. Clin. Oncol. 20, 3137–3148.

Sterlemann, V., Ganea, K., Liebl, C., Harbich, D., Alam, S., Holsboer, F., Müller, M.B., Schmidt, M.V., 2008. Long-term behavioral and neuroendocrine alterations following chronic social stress in mice: implications for stress-related disorders. Horm. Behav. 53, 386–394.

Stewart, K.L., 2016. Experimental Variables. In: Principles of Animal Research for Graduate and Undergraduate Students. Academic Press.

Stout, N.L., Fu, J.B., Silver, J.K., 2021. Prehabilitation is the gateway to better functional outcomes for individuals with cancer. J. Cancer Rehabilitat. 283–286.

Subramaniam, C.B., Wardill, H.R., Davies, M.R., Heng, V., Gladman, M.A., Bowen, J.M., 2023. 5-fluorouracil induces an acute reduction in neurogenesis and persistent neuroinflammation in a mouse model of the neuropsychological complications of chemotherapy. Mol. Neurobiol. 60, 1408–1424.

Sudo, M., Kano, Y., Ando, S., 2023. The effects of environmental enrichment on voluntary physical activity and muscle mass gain in growing rats. Front. Physiol. 14.

Sun, K.-T., Cheung, K.-K., Au, S.W.N., Yeung, S.S., Yeung, E.W., 2018. Overexpression of mechano-growth factor modulates inflammatory cytokine expression and macrophage resolution in skeletal muscle injury. Front. Physiol. 9.

Sun, K.T., Lam, J.W.Y., Tai, W.C.S., Lau, B.W.M., Yee, B.K., 2022. Within-subjects vs between-subjects co-variation of prepulse-elicited reaction and the diminution of startle to the succeeding pulse stimulus in the prepulse inhibition paradigm. Behav. Brain Res. 430, 113924.

Swerdlow, N.R., Braff, D.L., Geyer, M.A., 2016. Sensorimotor gating of the startle reflex: what we said 25 years ago, what has happened since then, and what comes next. J. Psychopharmacol. 30, 1072–1081.

Swerdlow, N.R., Eastvold, A., Uyan, K.M., Ploum, Y., Cadenhead, K., 2001. Matching strategies for drug studies of prepulse inhibition in humans. Behavioral Pharmacol. 12, 45–52.

Swerdlow, N.R., Geyer, M.A., 1993. Prepulse inhibition of acoustic startle in rats after lesions of the pedunculopontine tegmental nucleus. Behav. Neurosci. 107, 104–117.

Torres-Platas, S.G., Comeau, S., Rachalski, A., Bo, G.D., Cruceanu, C., Turecki, G., Giros, B., Mechawar, N., 2014. Morphometric characterization of microglial phenotypes in human cerebral cortex. J. Neuroinflammation 11.

van Praag, H., Kempermann, G., Gage, F.H., 2000. Neural consequences of enviromental enrichment. Nat. Rev. Neurosci. 1, 191–198.

VanderVeen, B.N., Cardaci, T.D., Madero, S.S., McDonald, S.J., Bullard, B.M., Price, R.L., Carson, J.A., Fan, D., Murphy, E.A., 2022a. 5-Fluorouracil disrupts skeletal muscle immune cells and impairs skeletal muscle repair and remodeling. J. Appl. Physiol. 133, 834–849.

VanderVeen, B.N., Cardaci, T.D., McDonald, S.J., Madero, S.S., Unger, C.A., Bullard, B. M., Enos, R.T., Velázquez, K.T., Kubinak, J.L., Fan, D., 2022b. Obesity reduced survival with 5-fluorouracil and did not protect against chemotherapy-induced cachexia or immune cell cytotoxicity in mice. Cancer Biol. Ther. 23, 1–15.

VanderVeen, B.N., Sougiannis, A.T., Velazquez, K.T., Carson, J.A., Fan, D., Murphy, E.A., 2020. The Acute Effects of 5 Fluorouracil on Skeletal Muscle Resident and Infiltrating Immune Cells in Mice. Front. Physiol. 11.

Varty, G.B., Paulus, M.P., Braff, D.L., Geyer, M.A., 2000. Environmental enrichment and isolation rearing in the rat: effects on locomotor behavior and startle response plasticity. Biol. Psychiatry 47, 864–873.

Vidal-Itriago, A., Radford, R.A.W., Aramideh, J.A., Maurel, C., Scherer, N.M., Don, E.K., Lee, A., Chung, R.S., Graeber, M.B., Morsch, M., 2022. Microglia morphophysiological diversity and its implications for the CNS. Front. Immunol. 13.

Walker II, W.H., Meléndez-Fernández, O.H., Pascoe, J.L., Zhang, N., DeVries, A.C., 2020. Social enrichment attenuates chemotherapy induced pro-inflammatory cytokine production and affective behavior via oxytocin signaling. Brain Behav. Immun. 89, 451–464.

Wang, Q., Wang, Y., Tian, Y., Li, Y., Han, J., Tai, F., Jia, R., 2024. Social environment enrichment alleviates anxiety-like behavior in mice: Involvement of the dopamine system. Behav. Brain Res. 456, 114687.

WHO, 2020. Model Lists of essential medicines (EML): Fluorouracil. Available: https://list.essentialmeds.org/?query=fluorouracil [Accessed 15 March 2024].

Winocur, G., 2017. Chemotherapy and cognitive impairment: An animal model approach. Canad. J. Exp. Psychol./Revue Canadienne De Psychologie Expérimentale 71, 265–273.

Winocur, G., Henkelman, M., Wojtowicz, J.M., Zhang, H., Binns, M.A., Tannock, I.F., 2012. The effects of chemotherapy on cognitive function in a mouse model: a prospective study. Clin. Cancer Res. 18, 3112–3121.

Winocur, G., Wojtowicz, J.M., Merkley, C.M., Tannock, I.F., 2016. Environmental enrichment protects against cognitive impairment following chemotherapy in an animal model. Behav. Neurosci. 130, 428–436.

Wittmann, M., Vollmer, T., Schweiger, C., Hiddemann, W., 2006. The relation between the experience of time and psychological distress in patients with hematological malignancies. Pall Supp Care 4, 357–363.

Wolff, B.S., Allen, H.R., Feng, L.R., Saligan, L.N., 2022. BDNF Val66Met Polymorphism Reduces the Fatigue-Like Effects of 5-Fluorouracil on Voluntary Wheel-Running Activity in Mice. Front. Behav. Neurosci. 16.

Wood, N.I., Carta, V., Milde, S., Skillings, E.A., McAllister, C.J., Ang, Y.L.M., Duguid, A., Wijesuriya, N., Afzal, S.M., Fernandes, J.X., 2010. Responses to environmental enrichment differ with sex and genotype in a transgenic mouse model of Huntington's Disease. PLoS One 5, e9077.

Xiao, R., Ali, S., Caligiuri, M.A., Cao, L., 2021. Enhancing Effects of Environmental Enrichment on the Functions of Natural Killer Cells in Mice. Front. Immunol. 12.

Xiao, S., Qin, D., Hou, X., Tian, L., Yu, Y., Zhang, R., Lyu, H., Guo, D., Chen, X.-Z., Zhou, C., 2023. Cellular senescence: a double-edged sword in cancer therapy. Front. Oncol. 13.

Xu, H., Gelyana, E., Rajsombath, M., Yang, T., Li, S., Selkoe, D., 2016. Environmental enrichment potently prevents microglia-mediated neuroinflammation by human amyloid -protein oligomers. J. Neurosci. 36, 9041–9056.

Yao, Z., Murali, B., Ren, Q., Luo, X., Faget, D.V., Cole, T., Ricci, B., Thotala, D., Monahan, J., van Deursen, J.M., 2020. Therapy-Induced Senescence Drives Bone Loss 80, 1171–1182.

Yee, B.K., Chang, D.T., Feldon, J., 2004. The effects of dizocilpine and phencyclidine on prepulse inhibition of the acoustic startle reflex and on prepulse-elicited reactivity in C57BL6 mice. Neuropsychopharmacol 29, 1865–1877.

Young, K., Morrison, H., 2018. Quantifying microglia morphology from photomicrographs of immunohistochemistry prepared tissue using imageJ. JoVE.

Zhang, S., Liu, Y., Xiang, D., Yang, J., Liu, D., Ren, X., Zhang, C., 2018. Assessment of dose-response relationship of 5-fluorouracil to murine intestinal injury. Biomed. Pharmacother. 106, 910–916.

Zhang, Z., Lu, Y., Zhang, H., Dong, S., Wu, Y., Wang, S., Huang, A., Jiang, Q., Yin, S., 2024. Enriched environment ameliorates fear memory impairments induced by sleep deprivation via inhibiting PIEZO1/calpain/autophagy signaling pathway in the basal forebrain. CNS Neurosci Ther 30.

Zhu, X., Grace, A.A., 2021. Prepubertal environmental enrichment prevents dopamine dysregulation and hippocampal hyperactivity in mam schizophrenia model rats. Biol. Psychiatry 89, 298–307.

Zubedat, S., Aga-Mizrachi, S., Cymerblit-Sabba, A., Ritter, A., Nachmani, M., Avital, A., 2015. Methylphenidate and environmental enrichment ameliorate the deleterious effects of prenatal stress on attention functioning. Stress 18, 280–288.